Structure preserving solver for Multi-dimensional Vlasov-Poisson type equations

Alain Blaustein

STRUCTURE PRESERVING SOLVER FOR MULTI-DIMENSIONAL VLASOV-POISSON TYPE EQUATIONS

Alain Blaustein[1]

Abstract. In [5], we have developed a discretization of the Vlasov-Poisson-Fokker-Planck model in the Hermite basis. This method allows for the treatment of different scales, ranging from collisionless regimes where we recover Vlasov-Poisson dynamics to highly collisional situations where the plasma behaves like a fluid. Furthermore, this approach preserves the entropy and hypocoercivity structure of the model, which facilitates its numerical analysis.

However, it may not be efficient in high dimensions, as it requires solving large systems, with typical size $(N_x N_v)^d$, where N_x (resp. N_v) denotes the spatial (resp. velocity) mesh refinement. Here, we propose a splitting scheme that preserves the structure of the system while drastically reducing the computational effort. More precisely, we decompose the system into N_v^d structure preserving blocks, each of sizes N_x^d and with same sparsity structure. We rigorously prove its structure preserving properties and illustrate its computational efficiency throughout various simulations.

Contents

2010 *Mathematics Subject Classification.* Primary: 82C40, Secondary: 65N08, 65N35 .
Key words and phrases. Hermite spectral method; Vlasov-Poisson, Fokker-Planck.
[1]akb7016@psu.edu, Pennsylvania State University, Department of Mathematics and Huck Institutes, State College, PA 16802, USA.

1. Introduction

The Vlasov-Poisson-Fokker-Planck system provides a kinetic description of a gas constituted of charged particles, let us say electrons and heavy positive ions, interacting through a mean electrostatic field:

$$\begin{cases} \partial_t f \,+\, \boldsymbol{v}\cdot\nabla_{\boldsymbol{x}} f \,+\, \mathbf{E}\cdot\nabla_{\boldsymbol{v}} f \,=\, \nu\,\mathrm{div}_{\boldsymbol{v}}\left(\boldsymbol{v} f \,+\, T_0\,\nabla_{\boldsymbol{v}} f\right)\,, \\ \\ \mathbf{E} = -\nabla_{\boldsymbol{x}}\Phi \;\;;\;\; -\lambda\Delta_{\boldsymbol{x}}\Phi \,=\, \rho-\rho_i \;\;;\;\; \rho(t,\boldsymbol{x}) = \displaystyle\int_{\mathbb{R}^d} f(t,\boldsymbol{x},\boldsymbol{v})\mathrm{d}\boldsymbol{v}\,, \end{cases} \tag{1.1}$$

The system is completed with the following condition, which ensures uniqueness of the potential Φ

$$\int_{\mathbb{T}^d} \Phi(t,\boldsymbol{x})\,\mathrm{d}\boldsymbol{x} \,=\, 0\,. \tag{1.2}$$

In (1.1), $f(t,\boldsymbol{x},\boldsymbol{v})$ is the distribution of particles over the phase space $(\boldsymbol{x},\boldsymbol{v}) \in \mathbb{T}^d \times \mathbb{R}^d$ at time $t \geq 0$, where $d \geq 1$. Field interactions are taken into account thanks to a coupling between kinetic and Poisson equations (first and second line of (1.1) respectively). In the Poisson equation, λ determines the nature and strength of interactions: $\lambda > 0$ corresponds to the repulsive or Coulomb case whereas $\lambda < 0$ corresponds to the attractive or Newtonian case. The right-hand side of the Poisson equation features the macroscopic distribution of particles $\rho(t,\boldsymbol{x})$ as well as a fixed background density $\rho_i(\boldsymbol{x})$. The following compatibility condition is satisfied for all time $t \geq 0$

$$\int_{\mathbb{T}^d} \rho(t,\boldsymbol{x})\,\mathrm{d}\boldsymbol{x} \,=\, \int_{\mathbb{T}^d} \rho_i(\boldsymbol{x})\,\mathrm{d}\boldsymbol{x}$$

as soon as it is initially verified. Thermodynamic effects are taken into account thanks to a Fokker-Planck operator, on the right-hand side of the kinetic equation, where appears the collision frequency $\nu \geq 0$ of particles with a surrounding bath described by a spatially homogeneous temperature $T_0 > 0$. The case $\nu = 0$ corresponds to the collisionless regime.

A major challenge in the numerical simulation of kinetic equations in plasma physics is to numerically account for their multi-scale nature (quasi-neutrality, weakly/strongly collisional). This first difficulty comes with another: kinetic equations suffer from the infamous "curse of dimensionality". This expression refers to their resolution cost, as the distribution function acts in the high-dimensional phase space $\mathbb{R}^d_{\boldsymbol{x}} \times \mathbb{R}^d_{\boldsymbol{v}}$. Several numerical methods have been proposed for (1.1)-(1.2), we mention for instance [21, 27, 9, 10, 6, 24]. These numerical schemes are either deterministic or stochastic, with an effort to capture some physical phenomena associated to weakly collisional plasmas such as Landau damping or two-stream instability, occurring for short time range, before being canceled by collisions. More recently, dynamical low-rank algorithms have been proposed [15, 8], they decouple the dimensions of the phase space allowing to reduce the computational cost.
Furthermore, intense efforts have been deployed in order to preserve the hypocoercivity structure of continuous Vlasov equations [12, 26, 13, 23], at the discrete level [25, 20, 14, 3]. These approaches ensure that the long time dynamics of the continuous model are faithfully reproduced. In this context, we have developed a discretization of the Vlasov-Poisson-Fokker-Planck model in the Hermite basis [5] in dimension $d = 1$. This method allows for the treatment of different scales without any constraint on the time step since it is fully implicit in time. Furthermore, it preserves the entropy and hypocoercivity structure of the model, which facilitates its asymptotic and stability analysis. However, it may not be efficient in

high dimensions, as it requires solving large systems, with typical size $N_x^d \times N_v^d$, where N_x (resp. N_v) denotes the number of mesh point in position (resp. velocity). Therefore, we propose an efficient splitting scheme that preserves the structure of the system while reducing the computational effort in high dimensions.

When $\nu > 0$, the equilibrium state f_∞ of (1.1) is uniquely determined as follows

$$f_\infty(\boldsymbol{x}, \boldsymbol{v}) \;=\; \rho_\infty(\boldsymbol{x})\, \mathcal{M}(\boldsymbol{v})\,,$$

where $\mathcal{M}$ denotes the Maxwellian with temperature T_0

$$\mathcal{M}(\boldsymbol{v}) \;=\; \frac{1}{(2\pi\, T_0)^{d/2}}\, \exp\left(-\frac{|\boldsymbol{v}|^2}{2\, T_0}\right)$$

and where ρ_∞ solves

$$\left\{\begin{array}{l} \rho_\infty \;=\; \exp\left(-\dfrac{\Phi_\infty}{T_0}\right)\,, \\[2ex] -\lambda \Delta_x \Phi_\infty \;=\; \rho_\infty - \rho_i\,, \end{array}\right. \tag{1.3}$$

completed with the following condition

$$\int_{\mathbb{T}^d} \exp\left(-\frac{\Phi_\infty}{T_0}\right) \mathrm{d}\boldsymbol{x} \;=\; \int_{\mathbb{T}^d} \rho_i\, \mathrm{d}\boldsymbol{x}\,.$$

In order to design a well-balanced approximation for (1.1)-(1.2), we consider an equivalent reformulation in terms of quantities near equilibrium. Replacing Φ with $\Psi = \Phi - \Phi_\infty$ in (1.1)-(1.2), we find that f solves

$$\left\{\begin{array}{l} \partial_t f \;+\; \boldsymbol{v}\cdot\nabla_{\boldsymbol{x}} f \;-\; \nabla_{\boldsymbol{x}}\Phi_\infty\cdot\nabla_{\boldsymbol{v}} f \;-\; \nabla_{\boldsymbol{x}}\Psi\cdot\nabla_{\boldsymbol{v}} f \;=\; \nu\, \mathrm{div}_{\boldsymbol{v}}\left(\boldsymbol{v} f \;+\; T_0\, \nabla_{\boldsymbol{v}} f\right)\,, \\[2ex] -\lambda\Delta_{\boldsymbol{x}}\Psi \;=\; \rho - \rho_\infty \;\;;\;\; \rho(t,\boldsymbol{x}) = \displaystyle\int_{\mathbb{R}^d} f(t,\boldsymbol{x},\boldsymbol{v})\mathrm{d}\boldsymbol{v}\,, \end{array}\right. \tag{1.4}$$

completed with the condition

$$\int_{\mathbb{T}^d} \Psi(t,\boldsymbol{x})\, \mathrm{d}\boldsymbol{x} \;=\; 0\,. \tag{1.5}$$

When $\nu > 0$, the equilibrium to (1.4)-(1.5) is now characterized by (f_∞, Ψ_∞) where $\Psi_\infty \equiv 0$.

The key-estimate to prove the trend to equilibrium of solutions to (1.4)-(1.5) is given by

$$\frac{\mathrm{d}}{\mathrm{d}t}\mathcal{H}(f, f_\infty) \;=\; -\,\nu\, \mathcal{I}(f, f_\infty),$$

where $\mathcal{H}(f, f_\infty)$ stands for the free energy

$$\mathcal{H}(f, f_\infty) \;:=\; \int_{\mathbb{T}^d\times\mathbb{R}^d} \ln\left(\frac{f}{f_\infty}\right) f\, \mathrm{d}\boldsymbol{x}\, \mathrm{d}\boldsymbol{v} \;+\; \frac{\lambda}{2\, T_0}\, \|\, \nabla_x \Psi\, \|^2_{L^2(\mathbb{T}^d)}\,,$$

and $\mathcal{I}(f, f_\infty)$ is the entropy dissipation

$$\mathcal{I}(f, f_\infty) \;:=\; 4\, T_0 \int_{\mathbb{T}^d\times\mathbb{R}^d} \left|\nabla_v \sqrt{\frac{f}{f_\infty}}\right|^2 f_\infty\, \mathrm{d}\boldsymbol{x}\, \mathrm{d}\boldsymbol{v}\,.$$

When f is near the equilibrium f_∞, we may plug the following formal expansion into the free energy

$$f\, \ln\left(\frac{f}{f_\infty}\right) \;\underset{f\to f_\infty}{\sim}\; f - f_\infty \;+\; \frac{|f - f_\infty|^2}{2\, f_\infty}\,.$$

Using that mass is conserved for solutions to (1.4)-(1.5), we define a new functional, named the linearized free energy, as

$$\mathcal{E}(t) \;=\; \| f(t) - f_\infty \|^2_{L^2(f_\infty^{-1})} \;+\; \frac{\lambda}{T_0} \| \nabla_x \Psi(t) \|^2_{L^2(\mathbb{T}^d)} \,. \tag{1.6}$$

Unfortunately, this functional is not dissipated by the nonlinear system (1.4)-(1.5), but only by its linearized version given by

$$\begin{cases} \partial_t f \;+\; \boldsymbol{v} \cdot \nabla_{\boldsymbol{x}} f \;-\; \nabla_{\boldsymbol{x}} \Phi_\infty \cdot \nabla_{\boldsymbol{v}} f \;-\; \nabla_{\boldsymbol{x}} \Psi \cdot \nabla_{\boldsymbol{v}} f_\infty \;=\; \nu \, \mathrm{div}_{\boldsymbol{v}} \left(\boldsymbol{v} f \;+\; T_0 \, \nabla_{\boldsymbol{v}} f \right) \,, \\ -\lambda \Delta_{\boldsymbol{x}} \Psi \;=\; \rho - \rho_\infty \;\;;\;\; \rho(t, \boldsymbol{x}) = \displaystyle\int_{\mathbb{R}^d} f(t, \boldsymbol{x}, \boldsymbol{v}) \mathrm{d}\boldsymbol{v} \,, \end{cases} \tag{1.7}$$

completed with the condition

$$\int_{\mathbb{T}^d} \Psi(t, \boldsymbol{x}) \, \mathrm{d}\boldsymbol{x} \;=\; 0 \,. \tag{1.8}$$

This yields for the solution (f, Ψ) to (1.7)-(1.8)

$$\frac{1}{2} \frac{\mathrm{d}}{\mathrm{d}t} \mathcal{E}(t) \;=\; -\, \nu \, T_0 \int_{\mathbb{T}^d \times \mathbb{R}^d} \left| \nabla_v \left(\frac{f(t)}{f_\infty} \right) \right|^2 f_\infty \, \mathrm{d}\boldsymbol{x} \, \mathrm{d}\boldsymbol{v} \,. \tag{1.9}$$

2. Reformulation of the model

In this section, we introduce our numerical method. We follow the lines of our previous work for the one dimensional Vlasov-Poisson-Fokker-Planck equation [5] and then propose a discretization of the Poisson equation allowing to preserve the energy estimate for the linearized problem. Finally, we present an efficient time splitting scheme using an implicit procedure allowing to reduce the computational effort.

2.1. **Hermite decomposition for the velocity variable.** The family of Hermite's functions $(\Psi_{\boldsymbol{k}})_{\boldsymbol{k} \in \mathbb{N}^d}$ defined as

$$\Psi_{\boldsymbol{k}}(\boldsymbol{v}) \;=\; H_{\boldsymbol{k}} \left(\frac{\boldsymbol{v}}{\sqrt{T_0}} \right) \mathcal{M}(\boldsymbol{v}) \,,$$

constitutes an orthonormal system of $L^2\left(\mathcal{M}^{-1}\right)$, that is

$$\int_{\mathbb{R}} \Psi_{\boldsymbol{k}}(\boldsymbol{v}) \Psi_{\boldsymbol{l}}(\boldsymbol{v}) \mathcal{M}^{-1}(\boldsymbol{v}) \mathrm{d}\boldsymbol{v} \;=\; \delta_{\boldsymbol{k},\boldsymbol{l}} \,.$$

In the latter definition, $(H_{\boldsymbol{k}})_{\boldsymbol{k} \in \mathbb{N}^d}$ stands for the family of d-dimensional Hermite polynomials

$$H_{\boldsymbol{k}}\left(\boldsymbol{\xi}\right) \;=\; H_{k_1}\left(\xi_1\right) \times \cdots \times H_{k_d}\left(\xi_d\right) , \quad \forall \boldsymbol{\xi} \in \mathbb{R}^d \,.$$

Hermite polynomials are defined recursively as follows $H_{-1} = 0$, $H_0 = 1$ and

$$\xi \, H_k(\xi) \;=\; \sqrt{k} \, H_{k-1}(\xi) \;+\; \sqrt{k+1} \, H_{k+1}(\xi) \,, \quad \forall \, k \;\geq\; 0 \,.$$

Let us also point out that Hermite's polynomials verify the following relation

$$H_k'(\xi) \;=\; \sqrt{k} \, H_{k-1}(\xi) \,, \quad \forall \, k \;\geq\; 0 \,.$$

The Hermite system arises naturally in our context since it offers a simple discrete reformulation of the $L^2\left(f_\infty^{-1}\right)$-norm which appears in the key estimate (1.9), indeed it holds

$$\|f(t)\|^2_{L^2(f_\infty^{-1})} \;=\; \sum_{\boldsymbol{k} \in \mathbb{N}^d} \|C_{\boldsymbol{k}}(t)\|^2_{L^2(\rho_\infty^{-1})} \,,$$

where $C = (C_{\boldsymbol{k}})_{\boldsymbol{k}\in\mathbb{N}^d}$ stand for the Hermite components of f

$$f\,(t,\boldsymbol{x},\boldsymbol{v}) \;=\; \sum_{\boldsymbol{k}\in\mathbb{N}^d} C_{\boldsymbol{k}}\,(t,\boldsymbol{x})\;\Psi_{\boldsymbol{k}}(\boldsymbol{v})\,.$$

2.2. **Well-balanced system through spatial normalization.** As one can see in the latter relation, each term of the sequence $C = (C_k)_{k\in\mathbb{N}^d}$ naturally belongs to the weighted space $L^2\left(\rho_\infty^{-1}\right)$. From the numerical point of view, working in weighted spaces induces difficulties when it comes to integration by part. Hence, we normalize the Hermite coefficients by the steady state in order to get a well-balanced scheme [7, 16, 5, 4]

$$f\,(t,\boldsymbol{x},\boldsymbol{v}) \;=\; \sqrt{\rho}_\infty(\boldsymbol{x}) \sum_{k\in\mathbb{N}^d} D_{\boldsymbol{k}}\,(t,\boldsymbol{x})\,\Psi_{\boldsymbol{k}}(\boldsymbol{v})\,. \tag{2.1}$$

According to latter considerations, normalized Hermite coefficients $D = (D_{\boldsymbol{k}})_{\boldsymbol{k}\in\mathbb{N}^d}$ verify

$$\|f(t)\|^2_{L^2\left(f_\infty^{-1}\right)} \;=\; \sum_{k\in\mathbb{N}^d} \|D_{\boldsymbol{k}}(t)\|^2_{L^2\left(\mathbb{T}^d\right)}\,.$$

To sum up, normalized Hermite coefficients play a fundamental role in our analysis for two reasons: they offer a discrete reformulation of the key quantity $\mathcal{E}(t)$ given by (1.6) and they belong to the **unweighted** Lebesgue space $L^2\left(\mathbb{T}^d\right)$. There is another benefit coming out of this choice: thanks to the properties of Hermite polynomials, one can see that Hermite functions diagonalize the Fokker-Planck operator since it holds

$$\nabla_{\boldsymbol{v}}\cdot\left[\,\boldsymbol{v}\,\Psi_{\boldsymbol{k}} \,+\, T_0\,\nabla_{\boldsymbol{v}}\,\Psi_{\boldsymbol{k}}\,\right] \;=\; -\,|\boldsymbol{k}|\;\Psi_{\boldsymbol{k}}\,.$$

Taking advantage of the latter relation and using that $-\sqrt{\rho}_\infty\nabla_{\boldsymbol{x}}\Phi_\infty = 2T_0\nabla_{\boldsymbol{x}}\rho_\infty$, we reformulate the Vlasov equation in (1.4) within the Hermite framework

$$\partial_t D_{\boldsymbol{k}} \,+\, \sum_{\alpha=1}^{d}\sqrt{\boldsymbol{k}_\alpha}\left(\mathcal{A}_\alpha + \frac{\partial_{\boldsymbol{x}_\alpha}\Psi}{\sqrt{T_0}}\right) D_{\boldsymbol{k}-\boldsymbol{e}_\alpha} \,-\, \sqrt{\boldsymbol{k}_\alpha+1}\,\mathcal{A}^\star_\alpha\,D_{\boldsymbol{k}+\boldsymbol{e}_\alpha} \;=\; -\,\nu\,|\boldsymbol{k}|\,D_{\boldsymbol{k}}\,, \tag{2.2}$$

for all $\boldsymbol{k}\in\mathbb{N}^d$, where we set $\boldsymbol{e}_\alpha = (\delta_{\beta=\alpha})_{1\le\beta\le d}$ and $D_{\boldsymbol{k}-\boldsymbol{e}_\alpha} = 0$ whenever $\boldsymbol{k}_\alpha - 1 < 0$. In the latter system, operators $\mathcal{A}_\alpha$ and $\mathcal{A}^\star_\alpha$ are given by

$$\left\{\begin{array}{l} \mathcal{A}_\alpha\,u \;=\; +\sqrt{T_0}\,\partial_{\boldsymbol{x}_\alpha}u \,+\, \dfrac{\partial_{\boldsymbol{x}_\alpha}\Phi_\infty}{2\sqrt{T_0}}\,u \\[2ex] \mathcal{A}^\star_\alpha\,u \;=\; -\sqrt{T_0}\,\partial_{\boldsymbol{x}_\alpha}u \,+\, \dfrac{\partial_{\boldsymbol{x}_\alpha}\Phi_\infty}{2\sqrt{T_0}}\,u \end{array}\right. \quad,\quad \forall\alpha\in\{1,\cdots,d\}\,. \tag{2.3}$$

We refer to the latter formulation as the algebraic form of $(\mathcal{A}_\alpha,\mathcal{A}^\star_\alpha)$. The operators also admit the following entropic form

$$\left\{\begin{array}{l} \mathcal{A}_\alpha\,u \;=\; +\sqrt{T_0}\,\sqrt{\rho}_\infty\partial_{\boldsymbol{x}_\alpha}\left(\sqrt{\rho}_\infty^{-1}u\right) \\[2ex] \mathcal{A}^\star_\alpha\,u \;=\; -\sqrt{T_0}\sqrt{\rho}_\infty^{-1}\,\partial_{\boldsymbol{x}_\alpha}\left(\sqrt{\rho}_\infty\,u\right) \end{array}\right. \quad,\quad \forall\alpha\in\{1,\cdots,d\}\,. \tag{2.4}$$

In this framework, the equilibrium D_∞ to (2.5) is simply given by

$$D_{\infty,\boldsymbol{k}} \;=\; \left\{\begin{array}{ll} \sqrt{\rho}_\infty\,, & \text{if } \boldsymbol{k}=0, \\[1ex] 0, & \text{else.} \end{array}\right.$$

2.3. **Reformulation of the field.** In order to prepare the analysis of the model at the discrete level, we also rewrite the field contribution in (2.2) in terms of operators $\mathcal{A}_\alpha$. Our main motivation being to preserve the linearized energy estimate (1.9) at the discrete level. According to (2.4), it holds

$$\frac{\partial_{\boldsymbol{x}_\alpha}\Psi}{\sqrt{T_0}} = \frac{1}{T_0\sqrt{\rho_\infty}}\mathcal{A}_\alpha\left(\sqrt{\rho_\infty}\Psi\right),$$

for all $\alpha = 1, \cdots, d$. Plugging the latter identity in (2.2), we rewrite the full system (1.4) as a coupled system between normalized Hermite coefficients $D = (D_{\boldsymbol{k}})_{\boldsymbol{k}\in\mathbb{N}^d}$ and the field Ψ. After separating linear from non-linear terms, we obtain

$$\left\{\begin{array}{l} \partial_t D_{\boldsymbol{k}} + \mathcal{L}_{\boldsymbol{k}}[D,\Psi] + \mathcal{N}_{\boldsymbol{k}}[D,\Psi] = 0, \quad \forall \boldsymbol{k}\in\mathbb{N}^d, \\ \\ -\lambda\Delta_{\boldsymbol{x}}\Psi = \sqrt{\rho_\infty}D_{\boldsymbol{0}} - \rho_\infty, \end{array}\right. \tag{2.5}$$

where $\mathcal{L}_{\boldsymbol{k}}$ gathers linear terms and is given by

$$\mathcal{L}_{\boldsymbol{k}}[D,\Psi] = \sum_{\alpha=1}^{d}\left(\sqrt{\boldsymbol{k}_\alpha}\mathcal{A}_\alpha\left(\frac{\sqrt{\rho_\infty}}{T_0}\delta_{\boldsymbol{k},\boldsymbol{e}_\alpha}\Psi + D_{\boldsymbol{k}-\boldsymbol{e}_\alpha}\right) - \sqrt{\boldsymbol{k}_\alpha+1}\,\mathcal{A}_\alpha^\star D_{\boldsymbol{k}+\boldsymbol{e}_\alpha}\right) + \nu\,|\boldsymbol{k}|\,D_{\boldsymbol{k}},$$

whereas $\mathcal{N}_{\boldsymbol{k}}$ gathers non-linear terms and is given by

$$\mathcal{N}_{\boldsymbol{k}}[D,\Psi] = \sum_{\alpha=1}^{d}\frac{\sqrt{\boldsymbol{k}_\alpha}}{T_0\sqrt{\rho_\infty}}\mathcal{A}_\alpha\left(\sqrt{\rho_\infty}\Psi\right)\left(D_{\boldsymbol{k}-\boldsymbol{e}_\alpha} - D_{\infty,\boldsymbol{k}-\boldsymbol{e}_\alpha}\right),$$

for all $\boldsymbol{k}\in\mathbb{N}^d$, where we set $D_{\boldsymbol{k}-\boldsymbol{e}_\alpha} = 0$ whenever $\boldsymbol{k}_\alpha - 1 < 0$.

3. A class of spatial discretizations

In this section, we propose and analyze a class of semi-discrete scheme for the reformulation (2.5) of (1.4). We prove that the method preserves the structure of the linearized equation (1.7). Our discretization is based on a finite volume method to discretize the spatial variable in (2.5).

3.1. **Geometry of the grid.** To discretize the spatial domain, we consider an interval (a,b) and for each direction $\alpha = 1, \cdots, d$, a subdivision of the interval (a,b)

$$a = x^\alpha_{1/2} < x^\alpha_{3/2} < \ldots < x^\alpha_{j-1/2} < x^\alpha_{j+1/2} < \ldots < x^\alpha_{N_x-1/2} < x^\alpha_{N_x+1/2} = b,$$

for a given number of point $N_x\in\mathbb{N}^\star$. Our discretization of $\mathbb{T}_{a,b}$ is then given by the family of control volumes $(K_{\boldsymbol{j}})_{\boldsymbol{j}\in\mathcal{J}}$

$$K_{\boldsymbol{j}} = \prod_{\alpha=1}^{d}\left]x^\alpha_{\boldsymbol{j}_\alpha-1/2}, x^\alpha_{\boldsymbol{j}_\alpha+1/2}\right[,$$

indexed by the set

$$\mathcal{J} = \{\boldsymbol{j}\in\mathbb{N}^d,\ \boldsymbol{e}\le\boldsymbol{j}\le N_x\boldsymbol{e}\},$$

where $\boldsymbol{e} = \boldsymbol{e}_1 + \cdots + \boldsymbol{e}_d$. Furthermore, we denote by x^α_j the middle of $\left]x^\alpha_{j-1/2}, x^\alpha_{j+1/2}\right[$ so that the center of the control volume $K_{\boldsymbol{j}}$ is given by

$$\boldsymbol{x}_{\boldsymbol{j}} := x^1_{\boldsymbol{j}_1}\boldsymbol{e}_1 + \cdots + x^d_{\boldsymbol{j}_d}\boldsymbol{e}_d.$$

For all $\alpha = 1, \cdots, d$ and all $j = 1, ..., N_x$, we define

$$\Delta x_j^\alpha = x_{j+1/2}^\alpha - x_{j-1/2}^\alpha \,.$$

Hence, for all $\boldsymbol{j} \in \mathcal{J}$, the volume of $K_{\boldsymbol{j}}$ is given by

$$\Delta \boldsymbol{x}_{\boldsymbol{j}} = \prod_{\alpha=1}^{d} \Delta x_{\boldsymbol{j}_\alpha}^\alpha \,,$$

and we denote by $l^2(\mathcal{J})$ the discrete L^2-norm on our grid

$$\|u\|_{l^2(\mathcal{J})}^2 = \sum_{\boldsymbol{j}\in\mathcal{J}} |u_{\boldsymbol{j}}|^2 \, \Delta \boldsymbol{x}_j \,, \tag{3.1}$$

for all $u \in \mathbb{R}^{\mathcal{J}}$. Finally the grid refinement parameter $h > 0$ is defined as

$$h = \max_{1\le j\le N_x} \max_{1\le\alpha\le d} \Delta x_j^\alpha \,.$$

3.2. **Discrete operators for Vlasov and Poisson equations.** in this section, we define the class of discrete analogs of $\mathcal{A}$ that will be used in our scheme. We also define the class of discrete analogs of $\Delta_{\boldsymbol{x}}$ used to discretize the Poisson equation in (1.4).
To discretize $\mathcal{A}$, we start from a finite volume method for the gradient $\nabla_{\boldsymbol{x}}$. More precisely, we denote by ∇^h a given discrete gradient over the grid $(K_{\boldsymbol{j}})_{\boldsymbol{j}\in\mathcal{J}}$, that is

$$\nabla^h \,:\, (u_{\boldsymbol{j}})_{\boldsymbol{j}\in\mathcal{J}} \longmapsto \left(\nabla_{\boldsymbol{j}}^h u\right)_{\boldsymbol{j}\in\mathcal{J}} \,.$$

For $1 \le \alpha \le d$, we denote by ∂_α^h the discrete partial derivative induced by ∇^h, and by $\partial_\alpha^{h,\star}$ its adjoint operator in $l^2(\mathcal{J})$, that is

$$\sum_{\boldsymbol{j}\in\mathcal{J}} \partial_{\alpha,\boldsymbol{j}}^h u \, v_{\boldsymbol{j}} \, \Delta \boldsymbol{x}_{\boldsymbol{j}} = \sum_{\boldsymbol{j}\in\mathcal{J}} u_{\boldsymbol{j}} \, \partial_{\alpha,\boldsymbol{j}}^{h,\star} v \, \Delta \boldsymbol{x}_{\boldsymbol{j}} \,.$$

We suppose that ∇^h is linear

$$\nabla^h (u + v) = \nabla^h u + \nabla^h v \,. \tag{3.2}$$

Remark 3.1. *Since ∇^h is linear, it is canceled by constants*

$$\nabla^h (u)_{\boldsymbol{j}\in\mathcal{J}} = 0 \,,$$

for all $u \in \mathbb{R}$.

We also suppose that ∇^h is stable and consistent with $\nabla_{\boldsymbol{x}}$, that is

$$\left\{ \begin{array}{l} \sup\limits_{\boldsymbol{i}\in\mathcal{J}} \left| \partial_{\alpha,\boldsymbol{i}}^h \left(u(\boldsymbol{x}_{\boldsymbol{j}})\right)_{\boldsymbol{j}\in\mathcal{J}} \right| \le C \\ \sup\limits_{\boldsymbol{i}\in\mathcal{J}} \left| \partial_{\alpha,\boldsymbol{i}}^h \left(u(\boldsymbol{x}_{\boldsymbol{j}})\right)_{\boldsymbol{j}\in\mathcal{J}} - \partial_{\boldsymbol{x}_\alpha} u(\boldsymbol{x}_{\boldsymbol{i}}) \right| \le C\, h \end{array} \right. , \quad \forall \alpha \in \{1, \cdots, d\} \,, \tag{3.3}$$

for all $u \in \mathscr{C}^1\left(\mathbb{T}_{a,b}^d\right)$ and for some constant $C > 0$ depending only on u.
We now propose two discretizations of the operator $\mathcal{A}$, corresponding respectively to its algebraic (2.3) and entropic (2.4) forms. Consider an approximation $(\rho_{\infty,\boldsymbol{j}})_{\boldsymbol{j}\in\mathcal{J}}$ of the equilibrium state ρ_∞ defined in (1.3). Entropic and algebraic discretizations of $\mathcal{A}_\alpha$ are given by

$$\left\{ \begin{array}{l} \mathcal{A}_{\alpha,\boldsymbol{j}}^{\mathrm{en}} u = \sqrt{T_0}\sqrt{\rho}_{\infty,\boldsymbol{j}} \partial_{\alpha,\boldsymbol{j}}^h \left(\sqrt{\rho_\infty}^{-1} u\right) \\ \mathcal{A}_{\alpha,\boldsymbol{j}}^{\mathrm{al}} u = \sqrt{T_0} \left(\partial_{\alpha,\boldsymbol{j}}^h u - \sqrt{\rho}_{\infty,\boldsymbol{j}}^{-1} \, \partial_{\alpha,\boldsymbol{j}}^h \left(\sqrt{\rho}_\infty\right) u_{\boldsymbol{j}}\right) \end{array} \right. , \quad \forall \alpha \in \{1, \cdots, d\} \,. \tag{3.4}$$

These discretizations preserve the equilibrium state of the equation since it holds

$$\mathcal{A}_\alpha^{\mathrm{al}}\sqrt{\rho}_\infty = \mathcal{A}_\alpha^{\mathrm{en}}\sqrt{\rho}_\infty = 0\,. \tag{3.5}$$

Dual operators in $l^2(\mathcal{J})$ of each form are explicitly given by

$$\left\{\begin{array}{l} \mathcal{A}_{\alpha,\boldsymbol{j}}^{\mathrm{en},\star}u \;=\; \sqrt{T_0}\sqrt{\rho}_{\infty,\boldsymbol{j}}^{-1}\partial_{\alpha,\boldsymbol{j}}^{h,\star}\left(\sqrt{\rho}_\infty u\right) \\ \mathcal{A}_{\alpha,\boldsymbol{j}}^{\mathrm{al},\star}u \;=\; \sqrt{T_0}\left(\partial_{\alpha,\boldsymbol{j}}^{h,\star}u \;-\; \sqrt{\rho}_{\infty,\boldsymbol{j}}^{-1}\,\partial_{\alpha,\boldsymbol{j}}^{h}\sqrt{\rho}_\infty\, u_{\boldsymbol{j}}\right) \end{array}\right. , \quad \forall\alpha\in\{1,\cdots,d\}\,. \tag{3.6}$$

The following property is satisfied by $\mathcal{A}^\star$ but only holds true for the entropic discretization

$$\mathcal{A}_\alpha^{\mathrm{en},\star}\sqrt{\rho}_\infty^{-1} = 0\,.$$

To discretize the Laplacian operator in Poisson equation in (1.4), we consider a discrete gradient $\tilde{\nabla}^h$ which meets assumptions (3.2)-(3.3) and define

$$\tilde{\Delta}^h \;=\; -\tilde{\nabla}^{h,\star}\cdot\tilde{\nabla}^h\,. \tag{3.7}$$

3.3. **Semi discrete scheme.** We now turn to the discretization of (2.5). We fix a number of Hermite modes $N_H\in\mathbb{N}^\star$ in each direction $\alpha=1,\cdots,d$ and we denote by $D_{\boldsymbol{k}}^h(t) = (\mathcal{D}_{\boldsymbol{k},\boldsymbol{j}}(t))_{\boldsymbol{j}\in\mathcal{J}}$ the approximation of $D_{\boldsymbol{k}}(t)$, where the index $\boldsymbol{k}$ lies in

$$\mathcal{H} = \{\boldsymbol{k}\in\mathbb{N}^d\,,\,\boldsymbol{0}\le\boldsymbol{k}\le N_H\boldsymbol{e}\}\,,$$

and represents the $\boldsymbol{k}$-th mode of the Hermite decomposition, whereas $\mathcal{D}_{\boldsymbol{k},\boldsymbol{j}}(t)$ is an approximation of the mean value of $D_{\boldsymbol{k}}(t)$ over the cell $K_{\boldsymbol{j}}$ at time t.

First of all, the initial condition is discretized on each cell $K_{\boldsymbol{j}}$ by:

$$\mathcal{D}_{\boldsymbol{k},\boldsymbol{j}}^{\mathrm{in}} = \frac{1}{\Delta x_{\boldsymbol{j}}}\int_{K_{\boldsymbol{j}}} D_{\boldsymbol{k}}(t=0,\boldsymbol{x})\,\mathrm{d}\boldsymbol{x}, \quad \boldsymbol{j}\in\mathcal{J}\,.$$

In order to solve $D^h(t) = (\mathcal{D}_{\boldsymbol{k},\boldsymbol{j}}(t))_{(\boldsymbol{k},\boldsymbol{j})\in\mathcal{H}\times\mathcal{J}}$ at time $t>0$, we replace $(\mathcal{A}_\alpha)_{1\le\alpha\le d}$ in (2.5) by one of the two finite volume methods $(\mathcal{A}_\alpha^{\mathrm{en}})_{1\le\alpha\le d}$ or $\left(\mathcal{A}_\alpha^{\mathrm{al}}\right)_{1\le\alpha\le d}$ detailed in Section 3.2 and denote by $\left(\mathcal{A}_\alpha^h\right)_{1\le\alpha\le d}$ the chosen method. We also replace the Laplacian operator of the Poisson coupling in (2.5) by the discrete Laplacian operator $\tilde{\Delta}^h$ introduced in Section 3.2. After separating linear and non linear terms, this yields

$$\left\{\begin{array}{l} \partial_t D_{\boldsymbol{k}}^h \;+\; \mathcal{L}_{\boldsymbol{k}}^h\left[D^h,\Psi^h\right] \;+\; \mathcal{N}_{\boldsymbol{k}}^h\left[D^h,\Psi^h\right] \;=\; 0\,, \quad \forall\boldsymbol{k}\in\mathcal{H}\,, \\ \\ -\lambda\tilde{\Delta}^h\Psi^h \;=\; \sqrt{\rho}_\infty D_{\boldsymbol{0}}^h - \rho_\infty\,, \end{array}\right. \tag{3.8}$$

where, as in the continuous case, $\mathcal{L}_{\boldsymbol{k}}^h$ gathers linear terms and is given by

$$\mathcal{L}_{\boldsymbol{k}}^h\left[D^h,\Psi^h\right] = \sum_{\alpha=1}^d\left(\sqrt{\boldsymbol{k}}_\alpha\mathcal{A}_\alpha^h\left(\frac{\sqrt{\rho}_\infty}{T_0}\delta_{\boldsymbol{k},\boldsymbol{e}_\alpha}\Psi^h + D_{\boldsymbol{k}-\boldsymbol{e}_\alpha}^h\right) - \sqrt{\boldsymbol{k}_\alpha+1}\,\mathcal{A}_\alpha^{h,\star}D_{\boldsymbol{k}+\boldsymbol{e}_\alpha}^h\right) + \nu\,|\boldsymbol{k}|\,D_{\boldsymbol{k}}^h\,,$$

whereas $\mathcal{N}_{\boldsymbol{k}}^h$ gathers non-linear terms and is given by

$$\mathcal{N}_{\boldsymbol{k}}^h\left[D^h,\Psi^h\right] = \sum_{\alpha=1}^d\frac{\sqrt{\boldsymbol{k}_\alpha}}{T_0\sqrt{\rho}_\infty}\mathcal{A}_\alpha^h\left(\sqrt{\rho}_\infty\Psi^h\right)\left(D_{\boldsymbol{k}-\boldsymbol{e}_\alpha}^h - D_{\infty,\boldsymbol{k}-\boldsymbol{e}_\alpha}\right)\,,$$

for all $\boldsymbol{k}\in\mathcal{H}$, where we set $D_{\boldsymbol{k}-\boldsymbol{e}_\alpha}=0$ (*resp.* $D_{\boldsymbol{k}+\boldsymbol{e}_\alpha}=0$) whenever $\boldsymbol{k}_\alpha-1<0$ (*resp.* $\boldsymbol{k}_\alpha+1>N_H$).

3.4. **Properties of the scheme.** In this section, we prove that our method preserves the energy estimate (1.9) verified by the linearized equation (1.7). Indeed, we prove that the linearized energy estimate (1.9) is verified by the equation obtained from (3.8) keeping only linear terms, that is

$$\left\{\begin{array}{l} \partial_t D^h_{\boldsymbol{k}} + \mathcal{L}^h_{\boldsymbol{k}}\left[D^h, \Psi^h\right] = 0\,, \quad \forall \boldsymbol{k} \in \mathcal{H}\,, \\ \\ -\lambda \tilde{\Delta}^h \Psi^h = \sqrt{\rho}_\infty D^h_{\boldsymbol{0}} - \rho_\infty\,, \end{array}\right. \tag{3.9}$$

where $\mathcal{L}^h_{\boldsymbol{k}}$ was defined for all $\boldsymbol{k} \in \mathcal{H}$ below (3.8) as follows

$$\mathcal{L}^h_{\boldsymbol{k}}\left[D^h, \Psi^h\right] = \sum_{\alpha=1}^{d}\left(\sqrt{\boldsymbol{k}}_\alpha \mathcal{A}^h_\alpha\left(\frac{\sqrt{\rho}_\infty}{T_0}\delta_{\boldsymbol{k},\boldsymbol{e}_\alpha}\Psi^h + D^h_{\boldsymbol{k}-\boldsymbol{e}_\alpha}\right) - \sqrt{\boldsymbol{k}_\alpha + 1}\,\mathcal{A}^{h,\star}_\alpha D^h_{\boldsymbol{k}+\boldsymbol{e}_\alpha}\right) + \nu\,|\boldsymbol{k}|\,D^h_{\boldsymbol{k}}\,,$$

At the discrete level, the energy of a solution Ψ^h, $D^h = \left(D^h_{\boldsymbol{k}}\right)_{\boldsymbol{k}\in\mathcal{H}}$ to (3.9) is defined as

$$\mathcal{E}^h(t) = \sum_{\boldsymbol{k}\in\mathcal{H}}\left\|D^h_{\boldsymbol{k}}(t) - D_{\infty,\boldsymbol{k}}\right\|^2_{l^2(\mathcal{J})} + \frac{\lambda}{T_0}\left\|\tilde{\nabla}^h\Psi^h(t)\right\|^2_{l^2(\mathcal{J})}\,, \tag{3.10}$$

where the discrete $l^2(\mathcal{J})$ norm is given in (3.1). Estimate (1.9) ensures that this quantity is conserved in the collisionless regime $\nu = 0$ and dissipated when $\nu > 0$. Therefore, the following result ensures stability at the discrete level in the Coulomb case $\lambda < 0$.

Theorem 3.2. *Under assumptions (3.2)-(3.3), denote by $\left(\mathcal{A}^h_\alpha\right)_{1\le\alpha\le d}$ one of the two discretization proposed in (3.4) and consider the linear operators $\left(\mathcal{L}^h_{\boldsymbol{k}}\right)_{\boldsymbol{k}\in\mathcal{H}}$ defined below (3.8). Then, any solution Ψ^h, $D^h = \left(D^h_{\boldsymbol{k}}\right)_{\boldsymbol{k}\in\mathcal{H}}$ to (3.9) satisfies*

$$\mathcal{E}^h(t) = \mathcal{E}^h(0) - 2\,\nu\int_0^t\sum_{\boldsymbol{k}\in\mathcal{H}}|\boldsymbol{k}|\left\|D^h_{\boldsymbol{k}}(s) - D_{\infty,\boldsymbol{k}}\right\|^2_{l^2(\mathcal{J})}\,\mathrm{d}s\,,$$

for all time $t \in \mathbb{R}^+$, where $\mathcal{E}^h(t)$ is defined by (3.10).

Proof. To compute the time derivative of $\sum_{\boldsymbol{k}\in\mathcal{H}}\left\|D^h_{\boldsymbol{k}}(t) - D_{\infty,\boldsymbol{k}}\right\|^2_{l^2(\mathcal{J})}$, we take the $l^2(\mathcal{J})$ scalar product between $2\left(D^h_{\boldsymbol{k}}(t) - D_{\infty,\boldsymbol{k}}\right)$ and the first line of (3.9). After summing over all $\boldsymbol{k} \in \mathcal{H}$, we obtain

$$\frac{\mathrm{d}}{\mathrm{d}t}\sum_{\boldsymbol{k}\in\mathcal{H}}\left\|D^h_{\boldsymbol{k}}(t) - D_{\infty,\boldsymbol{k}}\right\|^2_{l^2(\mathcal{J})} = \mathcal{E}_1 + \mathcal{E}_2 + \mathcal{E}_3\,,$$

where $\mathcal{E}_1$, $\mathcal{E}_2$ and $\mathcal{E}_3$ are given as follows

$$\left\{\begin{array}{l} \mathcal{E}_1 = 2\,\nu\sum_{\boldsymbol{k}\in\mathcal{H}}|\boldsymbol{k}|\left\langle D^h_{\boldsymbol{k}}(t)\,,\, D^h_{\boldsymbol{k}}(t) - D_{\infty,\boldsymbol{k}}\right\rangle_{l^2(\mathcal{J})}\,, \\ \\ \mathcal{E}_2 = -2\sum_{\boldsymbol{k}\in\mathcal{H}}\sum_{\alpha=1}^{d}\left\langle\sqrt{\boldsymbol{k}}_\alpha\mathcal{A}^h_\alpha D^h_{\boldsymbol{k}-\boldsymbol{e}_\alpha}(t) - \sqrt{\boldsymbol{k}_\alpha+1}\,\mathcal{A}^{h,\star}_\alpha D^h_{\boldsymbol{k}+\boldsymbol{e}_\alpha}(t)\,,\, D^h_{\boldsymbol{k}}(t) - D_{\infty,\boldsymbol{k}}\right\rangle_{l^2(\mathcal{J})}\,, \\ \\ \mathcal{E}_3 = -2\sum_{\boldsymbol{k}\in\mathcal{H}}\sum_{\alpha=1}^{d}\left\langle\sqrt{\boldsymbol{k}}_\alpha\mathcal{A}^h_\alpha\left(\frac{\sqrt{\rho}_\infty}{T_0}\delta_{\boldsymbol{k},\boldsymbol{e}_\alpha}\Psi^h(t)\right)\,,\, D^h_{\boldsymbol{k}}(t) - D_{\infty,\boldsymbol{k}}\right\rangle_{l^2(\mathcal{J})}\,. \end{array}\right.$$

The first term corresponds to the dissipation due to the Fokker-Planck operator on the right hand side of (1.7). It actually has a signed contribution. Indeed, using that $D_{\infty,\boldsymbol{k}} = 0$

whenever $\boldsymbol{k} \neq \mathbf{0}$, we obtain

$$\mathcal{E}_1 \;=\; -2\,\nu \sum_{\boldsymbol{k}\in\mathcal{H}} |\boldsymbol{k}| \left\| D^h_{\boldsymbol{k}}(t) - D_{\infty,\boldsymbol{k}} \right\|^2_{l^2(\mathcal{J})} .$$

The second term $\mathcal{E}_2$ corresponds to the coupled contribution between free transport and the field $\nabla_{\boldsymbol{x}}\Phi_\infty$ to the $L^2\left(f_\infty^{-1}\right)$-distance between f and f_∞ in (1.7). We check that this contribution is zero. Indeed using (3.5) and the duality structure, we rewrite $\mathcal{E}_2$ as follows

$$\mathcal{E}_2 = -2 \sum_{\alpha=1}^{d} \sum_{\boldsymbol{k}\in\mathcal{H}} \left\langle \sqrt{\boldsymbol{k}_\alpha}\mathcal{A}^h_\alpha D^h_{\boldsymbol{k}-\boldsymbol{e}_\alpha} \,,\, D^h_{\boldsymbol{k}}(t) - D_{\infty,\boldsymbol{k}} \right\rangle_{l^2(\mathcal{J})} - \left\langle \sqrt{\boldsymbol{k}_\alpha + 1}\, D^h_{\boldsymbol{k}+\boldsymbol{e}_\alpha}(t) \,,\, \mathcal{A}^h_\alpha D^h_{\boldsymbol{k}}(t) \right\rangle_{l^2(\mathcal{J})} .$$

Then, we re-index the first term in the latter sum setting $\boldsymbol{k} \leftarrow \boldsymbol{k} - \boldsymbol{e}_\alpha$ and obtain

$$\mathcal{E}_2 = 2 \sum_{\alpha=1}^{d} \sum_{\boldsymbol{k}\in\mathcal{H}} \left\langle \sqrt{\boldsymbol{k}_\alpha}\mathcal{A}^h_\alpha D^h_{\boldsymbol{k}-\boldsymbol{e}_\alpha} \,,\, D_{\infty,\boldsymbol{k}} \right\rangle_{l^2(\mathcal{J})} ,$$

where we used that $D_{\boldsymbol{k}-\boldsymbol{e}_\alpha} = 0$ whenever $\boldsymbol{k}_\alpha$ is 0 and $D_{\boldsymbol{k}+\boldsymbol{e}_\alpha} = 0$ whenever $\boldsymbol{k}_\alpha$ is N_H. Since $D_{\infty,\boldsymbol{k}} = 0$ if $\boldsymbol{k} \neq \mathbf{0}$, we deduce

$$\mathcal{E}_2 = 0 \,.$$

The last term $\mathcal{E}_3$ corresponds to the contribution of the self-consistent electric field Ψ in (1.7), it rewrites as follows

$$\mathcal{E}_3 \;=\; -2 \sum_{\alpha=1}^{d} \left\langle \mathcal{A}^h_\alpha \left(\frac{\sqrt{\rho}_\infty}{T_0} \Psi^h(t) \right) \,,\, D^h_{\boldsymbol{e}_\alpha}(t) \right\rangle_{l^2(\mathcal{J})} \;=\; -2 \left\langle \frac{\sqrt{\rho}_\infty}{T_0} \Psi^h(t) \,,\, \sum_{\alpha=1}^{d} \mathcal{A}^{h,\star}_\alpha D^h_{\boldsymbol{e}_\alpha}(t) \right\rangle_{l^2(\mathcal{J})} ,$$

where we used that $D_{\infty,\boldsymbol{e}_\alpha} = 0$ for all $\alpha = 1, \cdots, d$. Then, we replace $\sum_{\alpha=1}^{d} \mathcal{A}^{h,\star}_\alpha D^h_{\boldsymbol{e}_\alpha}$ in the latter right-hand side according to the first line in (3.9) with $\boldsymbol{k} = \mathbf{0}$, that is

$$\mathcal{E}_3 \;=\; -2 \left\langle \frac{\sqrt{\rho}_\infty}{T_0} \Psi^h(t) \,,\, \partial_t D^h_{\mathbf{0}}(t) \right\rangle_{l^2(\mathcal{J})} .$$

Using this time the Poisson coupling in the second line of (3.9), we deduce

$$\mathcal{E}_3 \;=\; \frac{2\,\lambda}{T_0} \left\langle \Psi^h(t) \,,\, \partial_t \tilde{\Delta}^h \Psi^h(t) \right\rangle_{l^2(\mathcal{J})} .$$

According to the definition (3.7) of $\tilde{\Delta}^h$, we deduce

$$\mathcal{E}_3 \;=\; -\frac{\lambda}{T_0} \frac{\mathrm{d}}{\mathrm{d}t} \left\| \tilde{\nabla}^h \Psi^h(t) \right\|^2_{l^2(\mathcal{J})} .$$

To conclude this proof, we sum our our estimates on $\mathcal{E}_1$, $\mathcal{E}_2$ and $\mathcal{E}_3$, this yields

$$\frac{\mathrm{d}}{\mathrm{d}t} \sum_{\boldsymbol{k}\in\mathcal{H}} \left\| D^h_{\boldsymbol{k}}(t) - D_{\infty,\boldsymbol{k}} \right\|^2_{l^2(\mathcal{J})} \;=\; -2\,\nu \sum_{\boldsymbol{k}\in\mathcal{H}} |\boldsymbol{k}| \left\| D^h_{\boldsymbol{k}}(t) - D_{\infty,\boldsymbol{k}} \right\|^2_{l^2(\mathcal{J})} - \frac{\lambda}{T_0} \frac{\mathrm{d}}{\mathrm{d}t} \left\| \tilde{\nabla}^h \Psi^h(t) \right\|^2_{l^2(\mathcal{J})} .$$

We obtain the result integrating the latter relation between 0 and t. □

4. Fully discrete and structure preserving scheme

In this section, we present a fully discrete scheme for (1.4). Our motivations are twofold: computational efficiency and structure preservation. We propose a time splitting method which takes advantage of the variational structure of the problem and which enables to achieve both simultaneously. We present our method in dimension one for sake of clarity and then show how it can be generalized to any dimension $d \geq 2$ without difficulty.

4.1. **One dimensional case.** First of all, we consider a family of control volumes $(K_{\boldsymbol{j}})_{j\in\mathcal{J}}$ for $\mathbb{T}$ as defined in Section 3.1 and the operators $\left(\mathcal{A}^h, \mathcal{A}^{h,\star}\right)$ and $\left(\tilde{\partial}_x^h, \tilde{\partial}_x^{h,\star}\right)$ defined in Section 3.2. Then, we fix a number of Hermite modes $N_H \geq 1$. To discretize the time variable, we fix a time step Δt and we set $t^n = n\Delta t$ with $n \in \mathbb{N}$. Our time discretization of $\mathbb{R}^+$ is then given by the increasing sequence of $(t^n)_{n\in\mathbb{N}}$.
We apply an efficient time splitting scheme based on an implicit scheme avoiding to solve a high dimensional system. Indeed, we first solve the following system for (Ψ^{n+1}, D_0^{n+1}) and $D_1^{(1)}$ as

$$\left\{\begin{array}{l} \dfrac{D_0^{n+1} - D_0^n}{\Delta t} - \mathcal{A}^{h,\star}\, D_1^{(1)} = 0\,, \\[2ex] \dfrac{D_1^{(1)} - D_1^n}{\Delta t} + \mathcal{A}^h\, D_0^{n+1} + \mathcal{A}^h\left(\dfrac{\sqrt{\rho}_\infty}{T_0}\Psi^{n+1}\right) = 0\,, \\[2ex] \lambda\, \tilde{\partial}_x^{h,\star}\, \tilde{\partial}_x^h\, \Psi^{n+1} = \sqrt{\rho_\infty}\, D_0^{n+1} - \rho_\infty\,. \end{array}\right. \tag{4.1}$$

It allows us to get an approximation (Ψ^{n+1}, D_0^{n+1}) at time t^{n+1} whereas $D_1^{(1)}$ is an intermediate approximation. To compute higher order Hermite coefficients, we solve the following systems for each $k \geq 1$ such that $2k \leq N_H$

$$\left\{\begin{array}{l} \dfrac{D_{2k}^{(1)} - D_{2k}^n}{\Delta t} - \sqrt{2k+1}\,\mathcal{A}^{h,\star}\, D_{2k+1}^{(1)} = -\,2k\,\nu\, D_{2k}^{(1)}\,, \\[2ex] \dfrac{D_{2k+1}^{(1)} - D_{2k+1}^n}{\Delta t} + \sqrt{2k+1}\,\mathcal{A}^h\, D_{2k}^{(1)} = 0\,, \end{array}\right. \tag{4.2}$$

with $D_{2k+1}^{(1)} = 0$ when $2k+1 > N_H$. From this first stage, we get $(D_k^{(1)})_{N_H\geq k\geq 1}$ by only solving a linear systems of size $2\,N_x$. In the second step, we solve the following systems for each $k \geq 1$ such that $2k-1 \leq N_H$

$$\left\{\begin{array}{l} \dfrac{D_{2k-1}^{(2)} - D_{2k-1}^{(1)}}{\Delta t} - \sqrt{2k}\,\mathcal{A}^{h,\star}\, D_{2k}^{(2)} = -\,(2k-1)\,\nu\, D_{2k-1}^{(2)}\,, \\[2ex] \dfrac{D_{2k}^{(2)} - D_{2k}^{(1)}}{\Delta t} + \sqrt{2k}\,\mathcal{A}^h\, D_{2k-1}^{(2)} = 0\,. \end{array}\right. \tag{4.3}$$

Again $(D_k^{(2)})_{N_H\geq k\geq 1}$ is obtained as a solution of a linear system of size $2\,N_x$. Finally, using again a fully implicit Euler scheme, we compute for $k \geq 1$,

$$\frac{D_k^{n+1} - D_k^{(2)}}{\Delta t} + \mathcal{N}_k^h\left[D^{n+1}, \Psi^{n+1}\right] = 0\,, \tag{4.4}$$

and $D_k^{n+1} = 0$ when $k > N_H$.

We now make four crucial remarks regarding the computational cost associated to this method. First, we observe that since D_0^{n+1} and Ψ^{n+1} does not change during step (4.4), the system **is trivially invertible** and hence does not require any linear solver. Furthermore, we emphasize that the matrices associated to systems (4.1), (4.2) and (4.3) are **time independent** so that they only need to be inverted once at time $t = 0$. In practice, we compute their LU decomposition with the superLU library [11]. Infact, the inversion time is negligible due to two main reasons. On the one hand this splitting scheme allows us to compute an approximation Ψ^{n+1} and D_k^{n+1} by solving N_H linear and nonlinear systems of **small size** $2N_x$ instead of one big system of size $N_H\, N_x$. On the other hand, we benefit from the fact

that, except for system (4.1), all the systems have the **same sparsity pattern**. Indeed the matrices associated to systems (4.2) and (4.3) all take the form

$$\begin{pmatrix} (1+k\,\nu\Delta t)\,\mathbf{I}_{N_x} & -\sqrt{k+1}\Delta t\mathcal{A}^{h,\star} \\ \sqrt{k+1}\Delta t\mathcal{A}^h & \mathbf{I}_{N_x} \end{pmatrix},$$

where only parameter k varies. Therefore, we may re-use row and column permutations to compute the LU decomposition for all values of k. For these reasons, we expect that this approach drastically reduces the computational effort, particularly for high dimension problems.

We now highlight the structure preserving property of the method. More precisely, we prove that the linearized energy is preserved by the first three steps of the numerical method (4.1)-(4.4). Indeed, we define the discrete free energy of the solution $D^n = (D_k^n)_{0\le k\le N_H}$ to (4.1)-(4.4) as follows

$$\mathcal{E}^n \;=\; \|D^n - D_\infty\|_{l^2}^2 \;+\; \frac{\lambda}{T_0}\left\|\,\tilde{\partial}_x^h\,\Psi^n\,\right\|_{l^2(\mathcal{J})}^2, \tag{4.5}$$

where

$$\|D^n - D_\infty\|_{l^2}^2 \;=\; \sum_{k=0}^{N_H}\|D_k^n - D_{\infty,k}\|_{l^2(\mathcal{J})}^2\,, \quad \text{and} \quad \|D_k\|_{l^2(\mathcal{J})}^2 \;=\; \sum_{j\in\mathcal{J}}|\mathcal{D}_{k,j}|^2\Delta x_j\,,$$

and recall that $\mathcal{A}^h$ and $\mathcal{A}^{\star,h}$ are adjoint operators in $l^2(\mathcal{J})$. Then, we prove the following result

Theorem 4.1. *Consider the solution $(D^n)_{n\in\mathbb{N}}$ to (4.1)-(4.4) with $\mathcal{N}^h = 0$. The following discrete energy estimate holds for all $n \ge 0$*

$$\frac{\mathcal{E}^{n+1}-\mathcal{E}^n}{\Delta t} + \Delta t\,\mathcal{R}_h^n \;=\; -\,2\,\nu\sum_{k=0}^{\left\lfloor\frac{N_H}{2}\right\rfloor}\left(2k\left\|D_{2k}^{(1)}\right\|_{l^2(\mathcal{J})}^2 + (2k+1)\left\|D_{2k+1}^{(2)}\right\|_{l^2(\mathcal{J})}^2\right),$$

with $D_{2k+1}^{(2)} = 0$ if $2k+1 > N_H$, and where $\mathcal{R}_h^n$ is the following positive remainder due to numeric dissipation

$$\mathcal{R}_h^n \;=\; \frac{\lambda}{T_0}\left\|\,\tilde{\partial}_x^h\frac{\Psi^{n+1}-\Psi^n}{\Delta t}\,\right\|_{l^2(\mathcal{J})}^2 + \left\|\frac{D_0^{n+1}-D_0^n}{\Delta t}\right\|_{l^2(\mathcal{J})}^2$$
$$+\sum_{k=1}^{N_H}\left(\left\|\frac{D_k^{(2)}-D_k^{(1)}}{\Delta t}\right\|_{l^2(\mathcal{J})}^2 + \left\|\frac{D_k^{(1)}-D_k^n}{\Delta t}\right\|_{l^2(\mathcal{J})}^2\right).$$

Proof. We use the notation $D_0^{(1)} \overset{def}{=} D_0^{n+1}$ and $D^{(1)} \overset{def}{=} (D_k^{(1)})_{0\le k\le N_H}$ for convenience in this proof. We first decompose the variations of $\mathcal{E}^n$ between time step n and $n+1$ into two terms, each one corresponding to one step in the splitting

$$\frac{\mathcal{E}^{n+1}-\mathcal{E}^n}{\Delta t} = \frac{\mathcal{E}^{n+1}-\mathcal{E}^{(1)}}{\Delta t} + \frac{\mathcal{E}^{(1)}-\mathcal{E}^n}{\Delta t}\,,$$

where $\mathcal{E}^{(1)}$ is defined as

$$\mathcal{E}^{(1)} \;=\; \frac{\lambda}{T_0}\left\|\,\tilde{\partial}_x^h\Psi^{n+1}\,\right\|_{l^2(\mathcal{J})}^2 \;+\; \|D^{(1)} - D_\infty\|_{l^2}^2\,.$$

Let us first compute $\left(\mathcal{E}^{(1)} - \mathcal{E}^n\right)/\Delta t$. For each $k \in \{0, \dots, N_H\}$, we take the $l^2(\mathcal{J})$ scalar product between the equation on the D_k in (4.1) or (4.2) and $D_k^{(1)} - D_{\infty,k}$, and then sum over all k, this yields

$$\frac{1}{2\,\Delta t}\left(\left\|D^{(1)} - D_\infty\right\|_{l^2}^2 - \left\|D^n - D_\infty\right\|_{l^2}^2 + \left\|D^{(1)} - D^n\right\|_{l^2}^2\right) = \mathcal{I}_1 + \mathcal{I}_2 - \nu \sum_{k=1}^{\left\lfloor \frac{N_H}{2} \right\rfloor} 2k \left\|D_{2k}^{(1)}\right\|_{l^2(\mathcal{J})}^2 ,$$

where we used $D_{\infty,2k} = 0$ when $k \geq 1$ to obtain the dissipation term on the right hand side and where $\mathcal{I}_1$ and $\mathcal{I}_2$ are given by

(4.6)

$$\begin{cases} \mathcal{I}_1 := \displaystyle\sum_{k=0}^{\left\lfloor \frac{N_H}{2} \right\rfloor} \sqrt{2k+1}\left(\left\langle \mathcal{A}^{h,\star}\, D_{2k+1}^{(1)}\,,\, D_{2k}^{(1)} - D_{\infty,k}\right\rangle_{l^2(\mathcal{J})} - \left\langle \mathcal{A}^h\, D_{2k}^{(1)}\,,\, D_{2k+1}^{(1)} - D_{\infty,k}\right\rangle_{l^2(\mathcal{J})}\right), \\ \mathcal{I}_2 := -\left\langle \mathcal{A}^h\left(\dfrac{\sqrt{\rho}_\infty}{T_0}\Psi^{n+1}\right)\,,\, D_1^{(1)}\right\rangle_{l^2(\mathcal{J})} , \end{cases}$$

where $D_{2k+1}^{(1)}$ is set to $\mathbf{0}$ when $2k+1 > N_H$. The term $\mathcal{I}_2$ accounts for the contribution of the electric field whereas $\mathcal{I}_1$ gathers the other terms.

Since $\mathcal{A}^h$ and $\mathcal{A}^{\star,h}$ are adjoint operators in $l^2(\mathcal{J})$ and using that $\mathcal{A}^h\, D_{\infty,0} = 0$ and $\mathcal{A}^h\, D_{\infty,k} = 0$ when $k \geq 1$, we obtain

$$\mathcal{I}_1 = 0\,.$$

Furthermore, considering the first equation in (4.1), we find that $\mathcal{I}_2$ rewrites as follows

$$\mathcal{I}_2 = -\left\langle \frac{\sqrt{\rho}_\infty}{T_0}\Psi^{n+1}\,,\, \frac{D_0^{n+1} - D_0^n}{\Delta t}\right\rangle_{l^2(\mathcal{J})} .$$

Then, we replace $D_0^{n+1} - D_0^n$ in the latter relation according to the third line in (4.1), which yields

$$\mathcal{I}_2 = -\left\langle \frac{\sqrt{\rho}_\infty}{T_0}\Psi^{n+1}\,,\, \frac{\lambda}{\sqrt{\rho}_\infty}\,\tilde{\partial}_x^{h,\star}\,\tilde{\partial}_x^h\,\frac{\Psi^{n+1} - \Psi^n}{\Delta t}\right\rangle_{l^2(\mathcal{J})} .$$

Therefore, we deduce the following relation

$$\mathcal{I}_2 = -\frac{\lambda}{2\,\Delta t\, T_0}\left(\left\|\tilde{\partial}_x^h \Psi^{n+1}\right\|_{l^2(\mathcal{J})}^2 - \left\|\tilde{\partial}_x^h \Psi^n\right\|_{l^2(\mathcal{J})}^2 + \left\|\tilde{\partial}_x^h\left(\Psi^{n+1} - \Psi^n\right)\right\|_{l^2(\mathcal{J})}^2\right) .$$

Gathering these computations, we deduce

$$\frac{\mathcal{E}^{(1)} - \mathcal{E}^n}{\Delta t} + \mathcal{R}_h^{(1)} = -2\nu \sum_{k=1}^{\left\lfloor \frac{N_H}{2} \right\rfloor} 2k \left\|D_{2k}^{(1)}\right\|_{l^2(\mathcal{J})}^2 ,$$

where

$$\mathcal{R}_h^{(1)} = \frac{\lambda}{T_0}\left\|\tilde{\partial}_x^h \frac{\Psi^{n+1} - \Psi^n}{\Delta t}\right\|_{l^2(\mathcal{J})}^2 + \left\|\frac{D_0^{n+1} - D_0^n}{\Delta t}\right\|_{l^2(\mathcal{J})}^2 + \sum_{k=1}^{N_H}\left\|\frac{D_k^{(1)} - D_k^n}{\Delta t}\right\|_{l^2(\mathcal{J})}^2 .$$

Following the same procedure, we also obtain

$$\frac{\mathcal{E}^{n+1} - \mathcal{E}^{(1)}}{\Delta t} + \mathcal{R}_h^{(2)} = -2\nu \sum_{k=0}^{\left\lfloor \frac{N_H}{2} \right\rfloor} (2k+1) \left\|D_{2k+1}^{(2)}\right\|_{l^2(\mathcal{J})}^2 ,$$

where

$$\mathcal{R}_h^{(2)} = \sum_{k=1}^{N_H} \left\| \frac{D_k^{(2)} - D_k^{(1)}}{\Delta t} \right\|_{l^2(\mathcal{J})}^2 .$$

We conclude this proof taking the sum between the last two estimates

$$\frac{\mathcal{E}^{(1)} - \mathcal{E}^n}{\Delta t} + \mathcal{R}_h^n = -2\nu \sum_{k=0}^{\left\lfloor \frac{N_H}{2} \right\rfloor} \left(2k \left\| D_{2k}^{(1)} \right\|_{l^2(\mathcal{J})}^2 + (2k+1) \left\| D_{2k+1}^{(2)} \right\|_{l^2(\mathcal{J})}^2 \right) .$$

□

Now let us see how to adapt this splitting scheme in two dimension.

4.2. **Two dimensional case.** First of all, we consider a family of control volumes $(K_{\boldsymbol{j}})_{\boldsymbol{j}\in\mathcal{J}}$ for $\mathbb{T}^2$ as defined in Section 3.1 and the operators $\left(\mathcal{A}_1^h, \mathcal{A}_2^h, \mathcal{A}_1^{h,\star}, \mathcal{A}_2^{h,\star}\right)$ defined in Section 3.2. Then, we denote by $D_{\boldsymbol{k}}^n = (\mathcal{D}_{\boldsymbol{k},\boldsymbol{j}}^n)_{\boldsymbol{j}\in\mathcal{J}}$ the approximation of $D_{\boldsymbol{k}}$, at time $t^n = n\Delta t$, where the index $\boldsymbol{k}$ lies in

$$\mathcal{H} = \{\boldsymbol{k} \in \mathbb{N}^2 \,,\, \boldsymbol{0} \leq \boldsymbol{k} \leq N_H \boldsymbol{e}\} \,,$$

and represents the $\boldsymbol{k}$-th mode of the Hermite decomposition, whereas $\mathcal{D}_{\boldsymbol{k},\boldsymbol{j}}^n$ is an approximation of the mean value of $D_{\boldsymbol{k}}(t^n)$ over the cell $K_{\boldsymbol{j}}$ at time t^n. The initial condition is discretized on each cell $K_{\boldsymbol{j}}$ by:

$$\mathcal{D}_{\boldsymbol{k},\boldsymbol{j}}^{\text{in}} = \frac{1}{\Delta x_{\boldsymbol{j}}} \int_{K_{\boldsymbol{j}}} D_{\boldsymbol{k}}(t=0, \boldsymbol{x}) \, \mathrm{d}\boldsymbol{x}, \quad \boldsymbol{j} \in \mathcal{J} \,.$$

Furthermore, we consider the following partition of our Hermite grid $\mathcal{H}$

$$\mathcal{H} = \mathcal{H}_1 \sqcup \mathcal{H}_2 \sqcup \mathcal{H}_3 \,,$$

where the disjoint sets $\mathcal{H}_1, \mathcal{H}_2, \mathcal{H}_3$ are defined as follows

$$\begin{cases} \mathcal{H}_1 = (3\mathbb{Z}\,\boldsymbol{e}_1 + \mathbb{Z}\,(\boldsymbol{e}_1 + \boldsymbol{e}_2)) \cap \mathcal{H} \\ \mathcal{H}_2 = (\boldsymbol{e}_1 + 3\mathbb{Z}\,\boldsymbol{e}_1 + \mathbb{Z}\,(\boldsymbol{e}_1 + \boldsymbol{e}_2)) \cap \mathcal{H} \\ \mathcal{H}_3 = (2\boldsymbol{e}_1 + 3\mathbb{Z}\,\boldsymbol{e}_1 + \mathbb{Z}\,(\boldsymbol{e}_1 + \boldsymbol{e}_2)) \cap \mathcal{H} \end{cases} , \tag{4.7}$$

To discretize the Vlasov equation (3.8) at time time t^n for $n > 0$, our approach is based on a time splitting scheme, where we first split and solve the linearized system and then the remaining nonlinear part. The whole process includes four steps, the first three solve the linearized operators $\left(\mathcal{L}_{\boldsymbol{k}}^h\right)_{\boldsymbol{k}\in\mathcal{H}}$ whereas the last step solves the remaining non linear terms.

Let us first present step $i = 1$, for which we execute the following procedure for each $\boldsymbol{k} \in \mathcal{H}_1$ and first consider the case $\boldsymbol{k} = \mathbf{0}$ by solving the following system yields $\left(D_{\mathbf{0}}^{n+1}, D_{\boldsymbol{e}_1}^{(1)}, D_{\boldsymbol{e}_2}^{(1)}, \Psi^{n+1}\right)$

$$
\left\{
\begin{array}{l}
\dfrac{D_{\mathbf{0}}^{n+1} - D_{\mathbf{0}}^{n}}{\Delta t} \; - \; \mathcal{A}_1^{h,\star}\, D_{\boldsymbol{e}_1}^{(1)} \; - \; \mathcal{A}_2^{h,\star}\, D_{\boldsymbol{e}_2}^{(1)} \; = \; 0\,, \\[2ex]
\dfrac{D_{\boldsymbol{e}_1}^{(1)} - D_{\boldsymbol{e}_1}^{n}}{\Delta t} \; + \; \mathcal{A}_1^{h}\, D_{\mathbf{0}}^{n+1} \; + \; \mathcal{A}_1^{h}\left(\dfrac{\sqrt{\rho}_\infty}{T_0}\Psi^{n+1}\right) \; = \; 0\,, \\[2ex]
\dfrac{D_{\boldsymbol{e}_2}^{(1)} - D_{\boldsymbol{e}_2}^{n}}{\Delta t} \; + \; \mathcal{A}_2^{h} D_{\mathbf{0}}^{n+1} \; + \; \mathcal{A}_2^{h}\left(\dfrac{\sqrt{\rho}_\infty}{T_0}\Psi^{n+1}\right) \; = \; 0\,, \\[2ex]
-\lambda\, \tilde{\Delta}^h \Psi^{n+1} \; = \; \sqrt{\rho}_\infty D_{\mathbf{0}}^{n+1} - \rho_\infty\,,
\end{array}
\right.
\tag{4.8}
$$

Then for $\boldsymbol{k} \in \mathcal{H}_1 \setminus \{\mathbf{0}\}$, we solve

$$
\left\{
\begin{array}{l}
\dfrac{D_{\boldsymbol{k}}^{(1)} - D_{\boldsymbol{k}}^{n}}{\Delta t} \; - \; \sqrt{\boldsymbol{k}_1 + 1}\, \mathcal{A}_1^{h,\star}\, D_{\boldsymbol{k}+\boldsymbol{e}_1}^{(1)} \; - \; \sqrt{\boldsymbol{k}_2 + 1}\mathcal{A}_1^{h,\star}\, D_{\boldsymbol{k}+\boldsymbol{e}_2}^{(1)} \; = \; -\,\nu\, |\boldsymbol{k}| D_{\boldsymbol{k}}^{(1)}\,, \\[2ex]
\dfrac{D_{\boldsymbol{k}+\boldsymbol{e}_1}^{(1)} - D_{\boldsymbol{k}+\boldsymbol{e}_1}^{(1)}}{\Delta t} \; + \; \sqrt{\boldsymbol{k}_1 + 1}\mathcal{A}_1^{h}\, D_{\boldsymbol{k}}^{(1)} \; = \; 0\,, \\[2ex]
\dfrac{D_{\boldsymbol{k}+\boldsymbol{e}_2}^{(1)} - D_{\boldsymbol{k}+\boldsymbol{e}_2}^{n}}{\Delta t} \; + \; \sqrt{\boldsymbol{k}_2 + 1}\mathcal{A}_2^{h}\, D_{\boldsymbol{k}}^{(1)} \; = \; 0\,,
\end{array}
\right.
\tag{4.9}
$$

allowing to get an intermediate approximation $\left(D_{\boldsymbol{k}}^{(1)}\right)_{\boldsymbol{k}\in\mathcal{H}\setminus\{0\}}$. Then we pursue with the second ($i = 2$) and third ($i = 3$) stages for $\boldsymbol{k} \in \mathcal{H}_i$,

$$
\left\{
\begin{array}{l}
\dfrac{D_{\boldsymbol{k}}^{(i)} - D_{\boldsymbol{k}}^{(i-1)}}{\Delta t} \; - \; \sqrt{\boldsymbol{k}_1 + 1}\mathcal{A}_1^{h,\star}\, D_{\boldsymbol{k}+\boldsymbol{e}_1}^{(i)} \; - \; \sqrt{\boldsymbol{k}_2 + 1}\mathcal{A}_1^{h,\star}\, D_{\boldsymbol{k}+\boldsymbol{e}_2}^{(i)} \; = \; -\,\nu\, |\boldsymbol{k}| D_{\boldsymbol{k}}^{(i)}\,, \\[2ex]
\dfrac{D_{\boldsymbol{k}+\boldsymbol{e}_1}^{(i)} - D_{\boldsymbol{k}+\boldsymbol{e}_1}^{(i-1)}}{\Delta t} \; + \; \sqrt{\boldsymbol{k}_1 + 1}\mathcal{A}_1^{h}\, D_{\boldsymbol{k}}^{(i)} \; = \; 0\,, \\[2ex]
\dfrac{D_{\boldsymbol{k}+\boldsymbol{e}_2}^{(i)} - D_{\boldsymbol{k}+\boldsymbol{e}_2}^{(i-1)}}{\Delta t} \; + \; \sqrt{\boldsymbol{k}_2 + 1}\mathcal{A}_2^{h}\, D_{\boldsymbol{k}}^{(i)} \; = \; 0\,,
\end{array}
\right.
\tag{4.10}
$$

which yields $\left(D_{\boldsymbol{k}}^{(3)}\right)_{\boldsymbol{k}\in\mathcal{H}\setminus\{0\}}$. After completing these three first steps, we proceed to the fourth one, in which we solve the remaining non linear terms. To do so, we operate the following computations

$$
\frac{D_{\boldsymbol{k}}^{n+1} - D_{\boldsymbol{k}}^{(3)}}{\Delta t} \; + \; \mathcal{N}_{\boldsymbol{k}}^{h}\left[D^{n+1}, \Psi^{n+1}\right] \; = \; 0\,, \quad \forall \boldsymbol{k} \in \mathcal{H} \setminus \{\mathbf{0}\}\,.
\tag{4.11}
$$

We emphasize that since Ψ^{n+1} and $D_{\mathbf{0}}^{n+1}$ are kept constant, the latter system is trivially invertible and therefore does not require any nonlinear solver.

We emphasize that the comments made in the previous section regarding computational efficiency still hold in dimension two:

(1) since $D_{\mathbf{0}}^{n+1}$ and Ψ^{n+1} do not change along (4.11), the system **is trivially invertible** and hence does not require any linear solver ;

(2) the matrices associated to systems (4.8), (4.9) and (4.10) are **time independent** so that they only need to be inverted once at time $t = 0$;
(3) We solve N_H^2 linear and nonlinear systems of **small size** $3N_xN_y$ instead of one big system of size $N_H^2\, N_xN_y$;
(4) systems (4.9) and (4.10) have the **same sparsity pattern** and similar values. Indeed their associated matrices read as

$$\begin{pmatrix} (1+|\boldsymbol{k}|\,\nu\Delta t)\,\mathbf{I}_{N_xN_y} & -\sqrt{\boldsymbol{k}_1+1}\Delta t\mathcal{A}_1^{h,\star} & -\sqrt{\boldsymbol{k}_2+1}\Delta t\mathcal{A}_2^{h,\star} \\ \sqrt{\boldsymbol{k}_1+1}\Delta t\mathcal{A}_1^{h} & \mathbf{I}_{N_xN_y} & \mathbf{0} \\ \sqrt{\boldsymbol{k}_2+1}\Delta t\mathcal{A}_2^{h} & \mathbf{0} & \mathbf{I}_{N_xN_y} \end{pmatrix},$$

where only parameter $\boldsymbol{k}$ varies. Therefore, we may re-use previous inversions to compute the inverse for all values of $\boldsymbol{k}$.

For these reasons, we expect that this approach drastically reduces the computational effort.

We now highlight the structure preserving property of the scheme. More precisely, we prove that the linearized energy is preserved by the first three steps of the numerical method (4.8)-(4.11). Indeed, we define the discrete free energy of the solution $D^n = (D^n_{\boldsymbol{k}})_{\boldsymbol{k}\in\mathcal{H}}$ to (4.8)-(4.11) as follows

$$\mathcal{E}^n \;=\; \|D^n - D_\infty\|_{l^2}^2 \;+\; \frac{\lambda}{T_0}\left\|\,\tilde{\nabla}^h\Psi^n\,\right\|_{l^2(\mathcal{J})}^2, \tag{4.12}$$

where

$$\|D^n - D_\infty\|_{l^2}^2 \;=\; \sum_{\boldsymbol{k}\in\mathcal{H}} \|D^n_{\boldsymbol{k}} - D_{\infty,\boldsymbol{k}}\|_{l^2(\mathcal{J})}^2\,, \quad \text{and} \quad \|D_{\boldsymbol{k}}\|_{l^2(\mathcal{J})}^2 \;=\; \sum_{\boldsymbol{j}\in\mathcal{J}} |\mathcal{D}_{\boldsymbol{k},\boldsymbol{j}}|^2\Delta x_{\boldsymbol{j}}\,,$$

Then, we prove the following result

Theorem 4.2. *Consider the solution $(D^n)_{n\in\mathbb{N}}$ to (4.8)-(4.11) with $\mathcal{N}^h = 0$. The following discrete energy estimate holds for all $n \geq 0$*

$$\frac{\mathcal{E}^{n+1}-\mathcal{E}^n}{\Delta t} \;+\; \Delta t\,\mathcal{R}_h^n \;=\; -\,2\,\nu\sum_{i=1}^{3}\sum_{\boldsymbol{k}\in\mathcal{H}_i}|\boldsymbol{k}|\,\left\|D^{(i)}_{\boldsymbol{k}}\right\|_{l^2(\mathcal{J})}^2,$$

where $\mathcal{R}_h^n$ is the following positive remainder due to numeric dissipation

$$\mathcal{R}_h^n = \frac{\lambda}{T_0}\left\|\,\tilde{\nabla}^h\frac{\Psi^{n+1}-\Psi^n}{\Delta t}\,\right\|_{l^2(\mathcal{J})}^2 + \left\|\frac{D^{n+1}_{\mathbf{0}}-D^n_{\mathbf{0}}}{\Delta t}\right\|_{l^2(\mathcal{J})}^2$$

$$+\sum_{\boldsymbol{k}\in\mathcal{H}\setminus\{\mathbf{0}\}}\left(\left\|\frac{D^{(3)}_{\boldsymbol{k}}-D^{(2)}_{\boldsymbol{k}}}{\Delta t}\right\|_{l^2(\mathcal{J})}^2 + \left\|\frac{D^{(2)}_{\boldsymbol{k}}-D^{(1)}_{\boldsymbol{k}}}{\Delta t}\right\|_{l^2(\mathcal{J})}^2 + \sum_{k=1}^{N_H}\left\|\frac{D^{(1)}_{\boldsymbol{k}}-D^{n}_{\boldsymbol{k}}}{\Delta t}\right\|_{l^2(\mathcal{J})}^2\right).$$

Proof. This proof follows the same lines as the one for Theorem 4.1 and therefore, we do not detail it. □

5. Simulations

We now illustrate the robustness of our method through various simulations, both in space dimension one and two.

5.1. **Bump-on-tail instability.** We first consider the bump-on-tail instability problem with the initial distribution as

$$f(0,x,v) = f_b(v)(1+\kappa\cos(k\,n\,x))\,, \tag{5.1}$$

where the bump-on-tail distribution is

$$f_b(v) = \frac{n_p}{\sqrt{\pi}v_p}e^{-v^2/v_p^2} + \frac{n_b}{\sqrt{\pi}v_b}e^{-(v-v_d)^2/v_b^2}\,. \tag{5.2}$$

We choose a strong perturbation with $\kappa = 0.04$, $n = 3$ and $k = 2\pi/L$ with $L = 62$ and the other parameters are set to be $n_p = 0.9$, $n_b = 0.1$, $v_d = 4.5$, $v_p = \sqrt{2}$, $v_b = \sqrt{2}/2$. The computational domain is $[0, L] \times [-8, 8]$. These settings have been used in [19, Section 4.3] and [2]. For this case, we take the initial scaling function to be $\alpha_0 = 5/7$.

We first show the time evolution of the relative deviations of discrete mass, momentum and total energy in Figure 1 (a). Here, the errors on mass and total energy are up to machine precision whereas the momentum varies with respect to time up to 10^{-5}. We remind that our space discretization does not ensure conservation of momentum. We also plot the time evolution of the electric field in L^2 norm in Figure 1 (b). We compare them to the results obtained in in [2] as a reference solution. We can see these results have the same structure and they are similar to those in [2].

Finally we show the surface plots of the distribution function at $t = 30$, 40 and 50 in Figure 2. From the comparison of these two methods, we can find that at the beginning $t \leq 20$, the solutions are very close. But as time evolves, the solutions are moving in different phases.

$N_x \times N_H$	splitting (4.1)-(4.4) ($\Delta t = 0.025$)	fully implicit [5] ($\Delta t = 0.1$)
150×150	8 sec.	5 sec.
300×300	32 sec.	27 sec.
600×600	1 min. 8 sec.	5 min. 2 sec.
1200×1200	8 min. 48 sec.	75 min. 50

TABLE 1. Computational time for the splitting scheme (4.1)-(4.4) with $\Delta t = 0.025$ and for the fully implicit scheme [5] with $\Delta t = 0.1$.

5.2. **The evolution of a beam in 2D.** We now consider the evolution of a matched semi-Gaussian beam in a uniform focusing channel in the four dimensional phase space. In this case the Vlasov equation has the following form, for all $\mathbf{x} = (x, y)$, and $\mathbf{v} = (v_x, v_y)$,

$$\frac{\partial f}{\partial t} + \boldsymbol{v}\cdot\nabla_{\boldsymbol{x}} f + (\mathbf{E}+\mathbf{E}_{\text{ext}})\cdot\nabla_{\boldsymbol{v}} f = \nu\,\text{div}_{\boldsymbol{v}}\,(\boldsymbol{v} f + \nabla_{\boldsymbol{v}} f) \tag{5.3}$$

where $\nu = 10^{-5}$, $\mathbf{E}$ is the self-consistent electric field given by the Poisson equation and $\mathbf{E}_{\text{ext}}$ is a linear external electric field allowing to focalize the beam

$$\mathbf{E}_{\text{ext}}(\boldsymbol{x}) = -\omega_0^2\,\boldsymbol{x}.$$

The initial value of the distribution function is

$$f_0(x,y,v_x,v_y) = \frac{n_0}{(2\,\pi\,v_{th}^2)\,(\pi\,a^2)}\mathrm{e}^{-\frac{v_x^2+v_y^2}{2\,v_{th}^2}}, \quad \text{if } x^2 + \frac{y^2}{r_0^2} \leq a^2,$$

and $f_0(x,y,v_x,v_y) = 0$, else. Then, we take

$$v_{th}^2 = \omega^2 a^2/4.$$

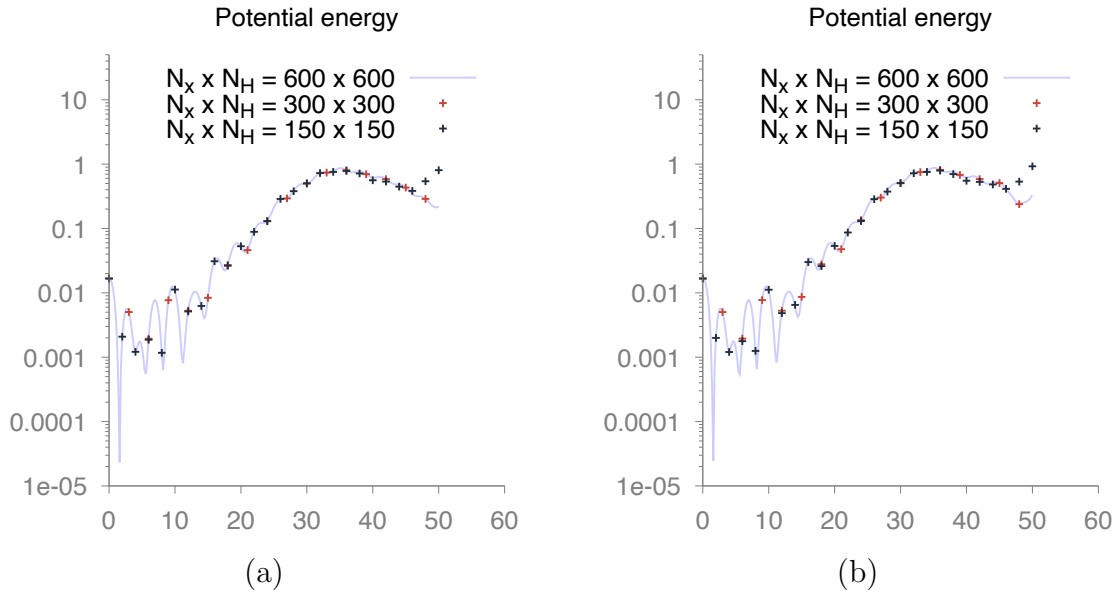

FIGURE 1. **Bump-on-tail instability:** time evolution of the electric field in L^2 norm in logarithmic value (a) using (4.1)-(4.4) with $\Delta t = 0.025$ and (b) the fully implicit scheme [5] with $\Delta t = 0.1$.

In this example, we have chosen ω and ω_0 such that the tune depression $\frac{\omega}{\omega_0}$=1/2. The beam density $n_0 = 1$.

Contour plots of the phase space projections as well as slices of the charge density and the electric field are given in the following figures (Figures 4 and 5). We notice that the beam at first becomes hollow, then regions of high density propagate to the core of the beam and out again, creating space charge waves. These waves are damped by phase mixing after a few lattice periods. Results seem to be very close to those obtained by the semi-lagrangian method [18].

6. Conclusion and perspectives

In this work, we propose an efficient time splitting scheme for the approximation of the high dimensional Vlasov-Poisson-Fokker-Planck model using Hermite expansion of the distribution function in velocity space. The strategy consists in identifying the general structure of the discretized Vlasov equations to design efficient schemes. More precisely, the idea is to "divide and conquer": rather than solving a large system, we solve many smaller and independent subsystems, while preserving the structure of the model. We have shown that our method preserves the structure structure of the model. To do so, we derived the energy estimate that holds for its linearized version.

Many interesting perspectives arise from this work. On the theoretical view point, an important continuation consists in extending our theoretical results, which apply for a linear coupling with the Poisson equation, to the nonlinear scheme by proving its asymptotic preserving properties and exponential trend towards equilibrium of discrete solutions. Another important continuation of this work is to incorporate nonlinear collisions to the model. Let us first observe that in [17], the Hermite spectral method is applied to a nonlinear Fokker-Planck operator conserving mass, momentum and energy. However, extending our analysis of the longtime regime at the discrete level to this case may require modifications and further investigations have to be done. L^2-hypocoercivity methods have been applied in the case of nonlinear BGK and linearized Boltzmann operators at the continuous level [22, 1], however

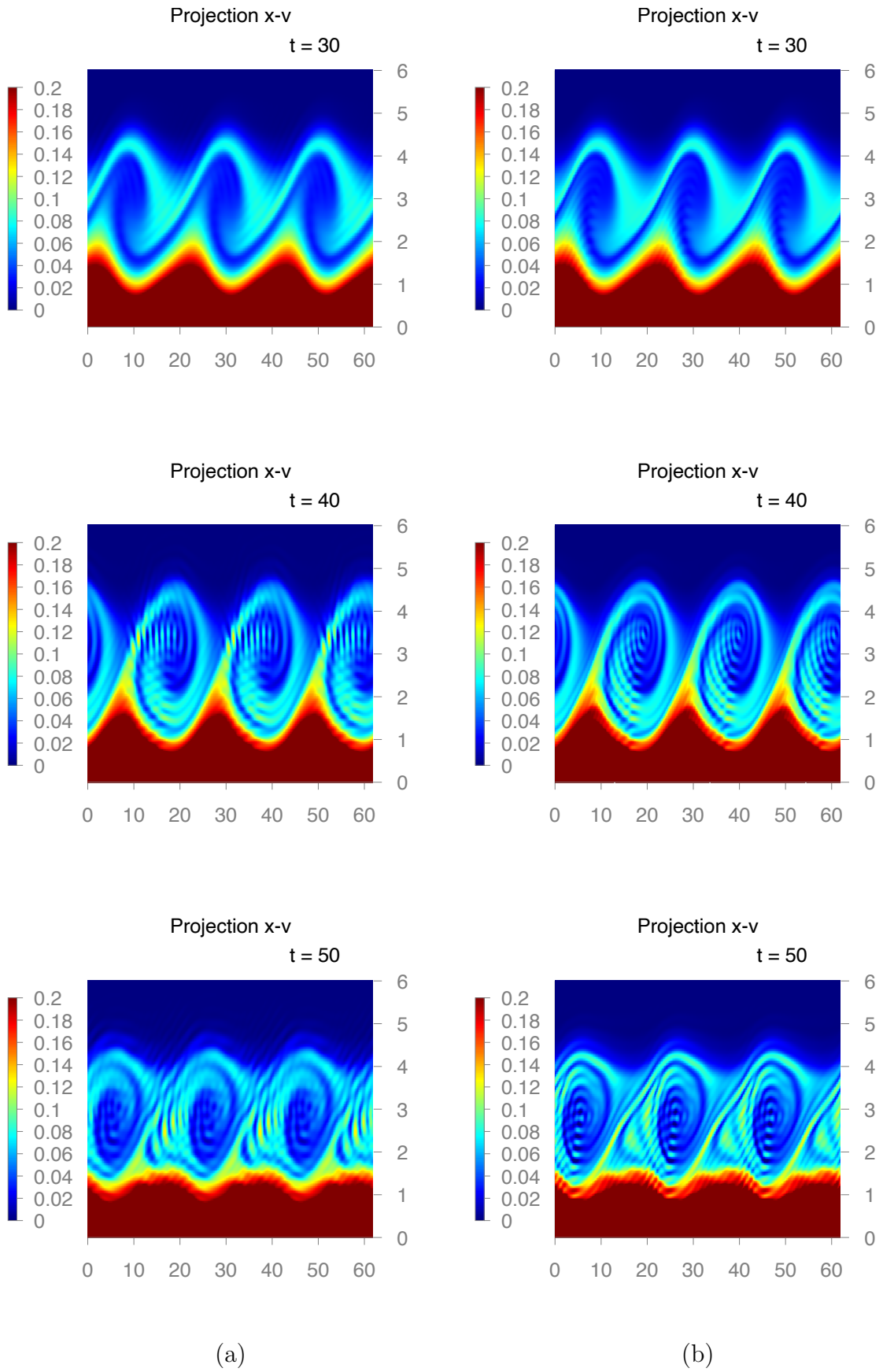

FIGURE 2. **Bump-on-tail instability:** Surface plot of the distribution function f at $t = 30$, 40 and 50 with $N_x \times N_H = 600 \times 600$ (a) using (4.1)-(4.4) with $\Delta t = 0.025$ and (b) the fully implicit scheme [5] with $\Delta t = 0.1$.

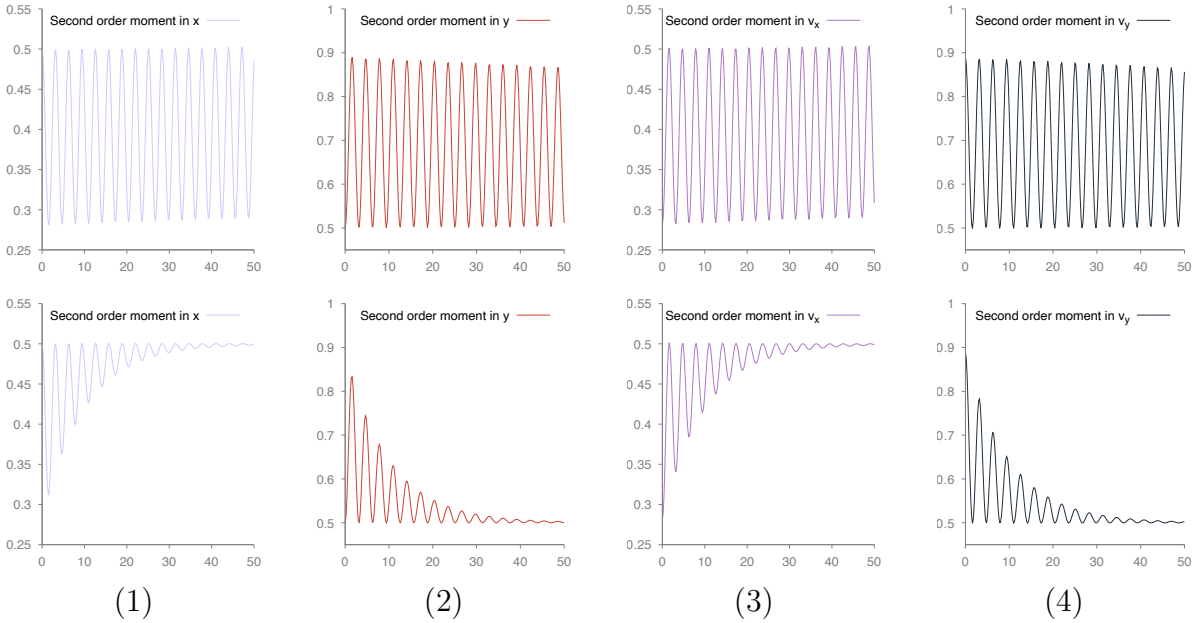

FIGURE 3. *Time development of moments of the distribution function for* $\nu = 10^{-5}$ *(top) and* $\nu = 10$ *(bottom).*

such analysis at the discrete level is not available in the literature in the framework of Hermite decomposition.

ACKNOWLEDGEMENT

REFERENCES

[1] F. Achleitner, A. Arnold, and E. A. Carlen. On multi-dimensional hypocoercive BGK models. *Kinet. Relat. Models*, 11(4):953–1009, 2018.

[2] M. Bessemoulin-Chatard and F. Filbet. On the stability of conservative discontinuous Galerkin/Hermite spectral methods for the Vlasov-Poisson system. *J. Comput. Phys.*, 451:Paper No. 110881, 28, 2022.

[3] M. Bessemoulin-Chatard, M. Herda, and T. Rey. Hypocoercivity and diffusion limit of a finite volume scheme for linear kinetic equations. *Math. Comp.*, 89(323):1093–1133, 2020.

[4] A. Blaustein and F. Filbet. On a discrete framework of hypocoercivity for kinetic equations. *Math. Comp.*, 93(345):163–202, 2024.

[5] A. Blaustein and F. Filbet. A structure and asymptotic preserving scheme for the Vlasov-Poisson-Fokker-Planck model. *J. Comput. Phys.*, 498:Paper No. 112693, 2024.

[6] J. A. Carrillo, L. Wang, W. Xu, and M. Yan. Variational Asymptotic Preserving Scheme for the Vlasov–Poisson–Fokker–Planck System. *Multiscale Modeling & Simulation*, 19(1):478–505, 2021.

[7] C. Chainais-Hillairet and M. Herda. Large-time behaviour of a family of finite volume schemes for boundary-driven convection-diffusion equations. *IMA J. Numer. Anal.*, 40(4):2473–2504, 2020.

[8] J. Coughlin and J. Hu. Efficient dynamical low-rank approximation for the Vlasov-Ampère-Fokker-Planck system. *J. Comput. Phys.*, 470:Paper No. 111590, 20, 2022.

[9] A. Crestetto, N. Crouseilles, and M. Lemou. Kinetic/fluid micro-macro numerical schemes for Vlasov-Poisson-BGK equation using particles. *Kinet. Relat. Models*, 5(4):787–816, 2012.

[10] P. Degond and F. Deluzet. Asymptotic-preserving methods and multiscale models for plasma physics. *J. Comput. Phys.*, 336:429–457, 2017.

[11] J. W. Demmel, S. C. Eisenstat, J. R. Gilbert, X. S. Li, and J. W. H. Liu. A supernodal approach to sparse partial pivoting. *SIAM J. Matrix Analysis and Applications*, 20(3):720–755, 1999.

[12] L. Desvillettes and C. Villani. On the trend to global equilibrium in spatially inhomogeneous entropy-dissipating systems: the linear Fokker-Planck equation. *Comm. Pure Appl. Math.*, 54(1):1–42, 2001.

[13] J. Dolbeault, C. Mouhot, and C. Schmeiser. Hypocoercivity for linear kinetic equations conserving mass. *Transactions of the American Mathematical Society*, 367(6):3807–3828, 2015.

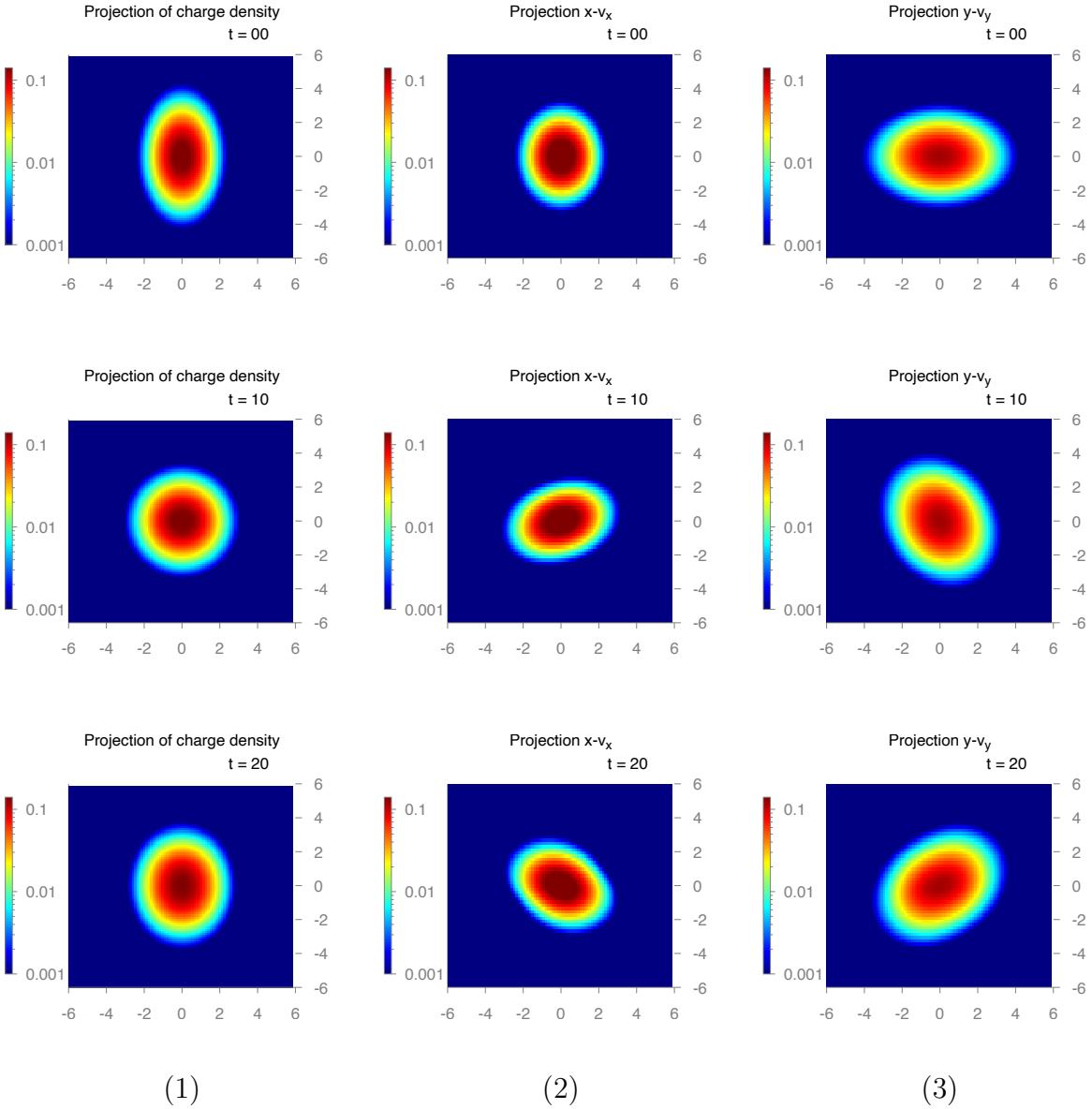

FIGURE 4. *Time development of (1) charge density, (2) x-v_x projection (3) y-v_y projection for $\nu = 10^{-5}$.*

[14] G. Dujardin, F. Hérau, and P. Lafitte. Coercivity, hypocoercivity, exponential time decay and simulations for discrete fokker–planck equations. *Numerische Mathematik*, 144(3):615–697, 2020.

[15] L. Einkemmer, J. Hu, and Y. Wang. An asymptotic-preserving dynamical low-rank method for the multi-scale multi-dimensional linear transport equation. *J. Comput. Phys.*, 439:Paper No. 110353, 21, 2021.

[16] F. Filbet and M. Herda. A finite volume scheme for boundary-driven convection-diffusion equations with relative entropy structure. *Numer. Math.*, 137(3):535–577, 2017.

[17] F. Filbet and C. Negulescu. Fokker-Planck multi-species equations in the adiabatic asymptotics. *J. Comput. Phys.*, 471:Paper No. 111642, 2022.

[18] F. Filbet, E. Sonnendrücker, and P. Bertrand. Conservative numerical schemes for the Vlasov equation. *Journal of Computational Physics*, 172(1):166–187, 2001.

[19] F. Filbet and T. Xiong. Conservative Discontinuous Galerkin/Hermite Spectral Method for the Vlasov–Poisson System. *Commun. Appl. Math. Comput.*, 2020.

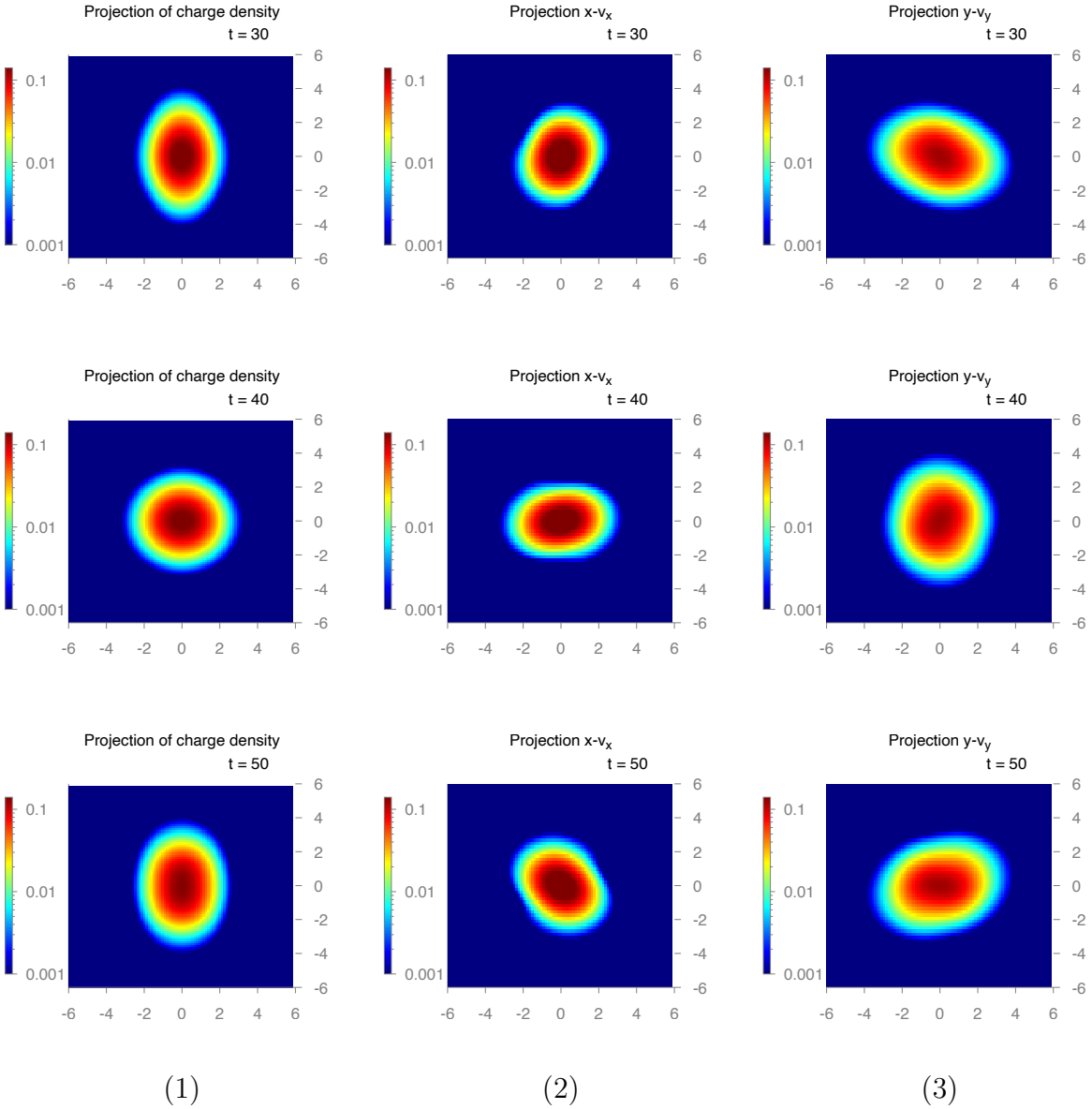

FIGURE 5. *Time development of (1) charge density, (2) x-v_x projection (3) y-v_y projection for $\nu = 10^{-5}$.*

[20] E. H. Georgoulis. Hypocoercivity-compatible finite element methods for the long-time computation of kolmogorov's equation. *SIAM Journal on Numerical Analysis*, 59(1):173–194, 2021.

[21] K. J. Havlak and H. D. Victory Jr. On deterministic particle methods for solving Vlasov–Poisson–Fokker–Planck systems. *SIAM journal on numerical analysis*, 35(4):1473–1519, 1998.

[22] F. Hérau. Hypocoercivity and exponential time decay for the linear inhomogeneous relaxation Boltzmann equation. *Asymptot. Anal.*, 46(3-4):349–359, 2006.

[23] F. Hérau. Introduction to hypocoercive methods and applications for simple linear inhomogeneous kinetic models. *arXiv preprint arXiv:1710.05588*, 2017.

[24] J. Jang, F. Li, J.-M. Qiu, and T. Xiong. High order asymptotic preserving DG-IMEX schemes for discrete-velocity kinetic equations in a diffusive scaling. *J. Comput. Phys.*, 281:199–224, 2015.

[25] A. Porretta and E. Zuazua. Numerical hypocoercivity for the kolmogorov equation. *Mathematics of Computation*, 86(303):97–119, 2017.

[26] C. Villani. Hypocoercivity. *Memoirs Amer. Math. Soc.*, 2009.

[27] S. Wollman and E. Ozizmir. Numerical approximation of the Vlasov–Poisson–Fokker–Planck system in one dimension. *Journal of Computational Physics*, 202(2):602–644, 2005.

Email address: `alain.blaustein@math.univ-toulouse.fr`